Journal of Power Sources 525 (2022) 231100

Contents lists available at ScienceDirect

Journal of Power Sources

journal homepage: www.elsevier.com/locate/jpowsour

Optimal probabilistic reliability-oriented planning of islanded microgrids considering hydrogen-based storage systems, hydrogen vehicles, and electric vehicles under various climatic conditions

Mehrdad Aslani [a,1], Amir Imanloozadeh [b,1], Hamed Hashemi-Dezaki [a,c,*], Maryam A. Hejazi [a,b], Mohammad Nazififard [b], Abbas Ketabi [a,b]

[a] Department of Electrical and Computer Engineering, University of Kashan, 6 km Ghotbravandi Blvd, 8731753153, Kashan, Iran
[b] Department of Energy Systems Engineering, School of Mechanical Engineering, University of Kashan, 6 km Ghotbravandi Blvd, 8731753153, Kashan, Iran
[c] Regional Innovational Center for Electrical Engineering (RICE), Faculty of Electrical Engineering, University of West Bohemia (UWB), 30100, Pilsen, Czech Republic

HIGHLIGHTS

- A novel optimal probabilistic planning for hydrogen-based microgrids.
- Considering the reliability constraints in the proposed stochastic method.
- Studying the proposed method in various climates.
- Investigating the EVs and HVs impacts on the optimal planning of MGs.
- More than 4.66% accuracy improvement by applying the proposed method.

GRAPHICAL ABSTRACT

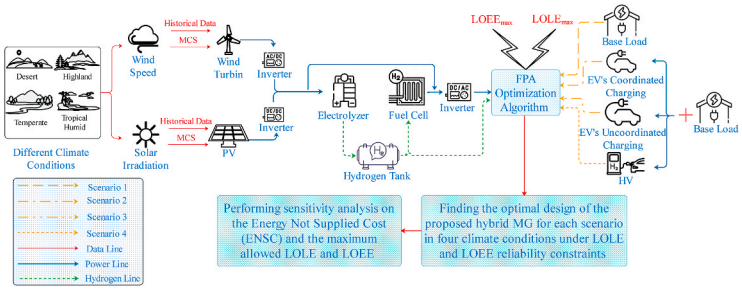

ARTICLE INFO

Keywords:
Optimal planning of microgrids
Hydrogen-based storage systems (HSSs)
Hydrogen vehicles (HVs)
Electric vehicles (EVs)
Probabilistic optimization problem
Monte Carlo simulation (MCS)

ABSTRACT

Much attention has been paid to the deployment of Hydrogen storage systems (HSSs) and Hydrogen vehicles (HVs) in the modernized energy system. However, a research gap exists in the literature about optimal probabilistic planning of microgrids (MGs) equipped with HSS, considering the uncertainties of renewable energy resources and electric vehicle (EV) and HV owners' behaviors. The main purpose of this research is to fill such a gap by developing a new probabilistic optimization problem to determine the capacity of Hydrogen-based MGs' sub-systems. Another contribution is to consider the reliability constraints and loss of energy cost (LOEC) in the MGs' total net present cost (TNPC). The Monte Carlo simulation (MCS) and Flower Pollination Algorithm (FPA) are used to model stochastic behaviors and solve the proposed probabilistic optimization problem. This paper studies different actual climates of Iran based on historical data, while various coordinated/uncoordinated charging modes of EVs and HVs are examined. Test results infer that a significant inaccuracy (more than 4.66% depends on the climate conditions and vehicle scenarios) occurs due to neglecting the uncertainties. The sensitivity analyses imply that the reliability constraints, LOEC, and their interactions might affect the MGs' optimal design.

* Corresponding author. Department of Electrical and Computer Engineering, University of Kashan, 6 km Ghotbravandi Blvd, 8731753153, Kashan, Iran.
E-mail addresses: m.aslani@grad.kashanu.ac.ir (M. Aslani), amir.imanloo@grad.kashanu.ac.ir (A. Imanloozadeh), hamed.hashemi@kashanu.ac.ir, hhashemi@fel.zcu.cz (H. Hashemi-Dezaki), mhejazi@kashanu.ac.ir (M.A. Hejazi), nazifi@kashanu.ac.ir (M. Nazififard), aketabi@kashanu.ac.ir (A. Ketabi).
[1] These authors have equal contributions to the paper.

https://doi.org/10.1016/j.jpowsour.2022.231100
Received 13 December 2021; Received in revised form 13 January 2022; Accepted 27 January 2022
Available online 11 February 2022

Nomenclature

Variables and Parameters

SCI	Hourly solar clearness index
η_{INV}	Inverter efficiency
E	Expected value function
$P_{INV\text{-}load}$	Inverter output power (kW)
P_{PV}	Photovoltaic (PV) output power (kW)
μ_{DD}	Mean value of driving distance
t	Time step (hour)
δ_{DD}	Standard deviation of driving distance
N_{PV}	Number of PV panels
μ_{AT}	Mean value of the arrival time
I_{PV}	PV output current (A)
δ_{AT}	Standard deviation of arrival time
V_{PV}	PV output voltage (V)
μ_{DT}	Mean departure time
c_{ws}	Shape parameter of Weibull cumulative density function (CDF)
k_{ws}	Scale parameter of Weibull cumulative density function (CDF)
N_v	Total number of vehicles
δ_{DT}	Standard deviation of departure time
$n_{i,F}$	Number of faulty components of the i-th type of elements
G/G_0	Solar irradiance/standard solar irradiance (kW/m^2)
u	Uniform distributed random number
p	A threshold for the switch probability variables
ws	Wind speed
n_v	Vehicle number
ws_{co}	Cut-off speed (m/s)
ws_{ci}	Cut-in speed (m/s)
P_{WT}	Wind turbine (WT) output power (kW)
P_{RES}	Available output power of the renewable energy sources (kW)
ws_{rated}	Rated wind speed (m/s)
N_{WT}	Number of wind turbines
P_{WT}^{Rated}	Wind turbine rated power (kW)
A_i	Availability of the i-th type of elements
T_c/T_a	Solar cell/ambient temperature (°C)
η_{PV}	PV efficiency
μ_{T_a}	Mean value of the solar ambient temperature
IS	Inverter state
σ_{T_a}	Standard deviation of ambient temperature
$TNPC$	Total net present cost (USD)
α/β	Parameters of the Beta probability distribution
NPC_{Com}	Net present cost for system components (USD)
PDF	Probability density function
NPC_{LOEE}	Net present cost of loss of load (USD)
CDF	Cumulative density function
C_I	Total investment cost (IC) (USD)
N_{OT}	Nominal operating temperature of PV cells (°C)
$C_{O\&M}$	Total operation and maintenance (O&M) cost (USD)
K_I	Current-temperature coefficient (A/°C)
$C_{O\&M}^{i}$	Operation and maintenance cost of the i-th type of elements (USD)
I_{sc}	PV short-circuit current (A)
C_{Rep}	Total replacement cost (RC) (USD)
V/V_{oc}	Output voltage and open-circuit voltage of PV modules (V)
C_{Rep}^{i}	Replacement cost of the i-th type of elements (USD)
K_V	Voltage temperature coefficient (V/°C)
$LOEE$	Loss of energy expected
η	Efficiency
$LOEE_{max}$	Maximum allowed loss of energy expected
η_{EL}	Electrolyzer efficiency
LC	Load curtailment
η_I	Electric current efficiency
PF_{LOEE}	Loss of load penalty factor
η_V	Voltage efficiency
$FPAI$	Iteration number of the flower pollination algorithm
$P_{EL\text{-}HT}$	Electrolyzer output power to hydrogen tank (HT) (kW)
$ENSC$	Energy not-supplied cost (USD/kWh)
$P_{RES\text{-}EL}$	Renewable source output power to electrolyzer (kW)
PWA	Capital annual recovery factor
E_{HT}	Stored energy in HT (kWh)
N_i	Number of the i-th component
$P_{HT\text{-}FC}$	HT output power to the fuel cell (FC) (kW)
ir	Real interest rate
E_{HV}	Load demand of hydrogen vehicle (HV) (kW)
ir_{nom}	Nominal interest rate
m_{HT}	Stored hydrogen mass (kg)
f	Annual inflation rate
HHV	High heat value (kWh/m^3)
y	Number of replacements
Δt	Time interval (hour)
L	Useful lifetime (year)
$P_{FC\text{-}INV}$	FC output power to the inverter (kW)
Γ	Gamma function
η_{FC}	FC efficiency
g^*	The best solution of any iteration of the flower pollination algorithm
$P_{RES\text{-}INV}$	Renewable source output power to the inverter (kW)
ε	A random variable with the uniform distribution in [0,1] for applying the local pollination
γ	Scale coefficient
x_l^{FPAI}	The l-the decision variable at the $FPAI$-the iteration of the flower pollination algorithm
$L(\lambda)$	Stair size
$LOLE$	Loss of load expected
$MCSI$	Iteration number of the Monte Carlo simulation
Pr	Probability function
$n_{WT,F}$	Number of failed WT units
$n_{PV,F}$	Number of the failed PV units
A_{WT}	Availability of WT units
A_{PV}	Availability of PV units
N_{MCS}	Maximum number of MCS iterations
A_{INV}	Availability of the inverter units
C_{PVs}	Investment cost of PV units (USD)
C_{WTs}	Investment cost of WT units (USD)
C_{EL}	Investment cost of the electrolyzer (USD)
C_{HT}	Investment cost of the Hydrogen tank (USD)
C_{FC}	Investment cost of the fuel cell (USD)
C_{INV}	Investment cost of the inverter (USD)
$C_{O\&M}^{PVs}$	Annual operation and maintenance cost of PV units
$C_{O\&M}^{WTs}$	Annual operation and maintenance cost of WT units
$C_{O\&M}^{EL}$	Annual operation and maintenance cost of the electrolyzer
$C_{O\&M}^{HT}$	Annual operation and maintenance cost of the Hydrogen tank
$C_{O\&M}^{FC}$	Annual operation and maintenance cost of the fuel cell
$C_{O\&M}^{INV}$	Annual operation and maintenance cost of the inverter
C_{Rep}^{PVs}	Replace cost of PV units
C_{Rep}^{WTs}	Replace cost of WT units
C_{Rep}^{EL}	Replace cost of the electrolyzer
C_{Rep}^{HT}	Replace cost of the Hydrogen tank
C_{Rep}^{FC}	Replace cost of the fuel cell
C_{Rep}^{INV}	Replace cost of the inverter
y_{PV}	Total number of PV replacements
y_{WT}	Total number of WT replacements

y_{EL}	Total number of electrolyzer replacements
y_{HT}	Total number of Hydrogen tank replacements
y_{FC}	Total number of fuel cell replacements
y_{INV}	Total number of inverter replacements
L_{PV}	Lifetime of PV units
L_{WT}	Lifetime of WT units
L_{EL}	Lifetime of the electrolyzer
L_{HT}	Lifetime of the Hydrogen tank
L_{FC}	Lifetime of the fuel cell
L_{INV}	Lifetime of the inverter
n_{H_2}	Amount of produced Hydrogen
V_{EL}^{0}	Reversible potential
F_{EL}	Faraday constant
V_{EL}^{Ohm}	Ohmic voltage
J_{EL}	Current density
$V_{EL}^{Act,a}$	Activation overpotential of anode
V_{EL}	Overpotential
$V_{EL}^{Act,c}$	Activation overpotential of cathode
E_{EL}^{elec}	Required electricity for Hydrogen production

Abbreviations

PV	Photovoltaic
WT	Wind Turbine
EL	Electrolyzer
HT	Hydrogen Tank
FC	Fuel Cell
TNPC	Total Net Present Cost
PSO	Particle Swarm Optimization
WM	Worst Month
HSS	Hydrogen Storage System
RO	Robust Optimization
LPSP	Loss of Power Supply Probability
ESS	Energy Storage System
PHS	Pumped Hydro Storage
HEV	Hybrid Electric Vehicles
SC	Supercapacitor
DP	Dynamic Programming
ES	Energy Storage
AI	Artificial Intelligence
MILP	Mixed-Integer Linear Programming
DD	Driving Distance
AT	Arrival Time
O&M	Operation and Maintenance
LOEC	Loss of Energy Cost
LOLE	Loss of Load Expected
LOEE	Loss of Energy Expected
PHEV	Plug-in Hybrid Electric Vehicle
SCI	Solar Clearness Index
PEME	Polymer Electrolyte Membrane Electrolyzer
ANN	Artificial Neural Network
CFD	Computational Fluid Dynamics
OF	Objective Function
NPC	Net Present Cost
EV	Electric Vehicle
HV	Hydrogen Vehicle
MG	Micro Grid
GHG	Greenhouse Gas
DEG	Distributed Energy Generation
RES	Renewable Energy Sources
GWO	Grey Wolf Optimizer
YAM	Yearly Average Month
DPR	Demand Response Program
GAMS	General Algebraic Modeling System
GT	Game Theory
MGO	Micro Grid Operator
HFC	Hydrogen Fuel Cell
COE	Cost of Energy
V2G	Vehicle to Grid
FCHEV	Fuel Cell Hybrid Electric Vehicle
RET	Region Elimination Technique
TLBO	Teaching-Learning Based Optimization
FPA	Flower Pollination Algorithm
DT	Departure Time
IC	Investment Cost
RC	Replacement Cost
MCS	Monte Carlo Simulation
ENSC	Energy Not Supplied Cost
PEMFC	Proton Exchange Membrane Fuel Cell
PDF	Probability Density Function
CDF	Cumulative Density Function
PHSS	Pumped Hydro Storage System
MINLP	Mixed-Integer Nonlinear Programming
GA	Genetic Algorithm
SOE	State of Energy
ABC	Artificial Bee Colony

1. Introduction

1.1. Motivation and incitement

The global energy demand is steadily increasing worldwide, and it has been reported that the energy sector would be one of the essential economic contributors to investments and job positions [1,2]. Also, exhausting fossil fuel-based energy generation technologies has received much attention [3–5]. Hence, a great deal of attention has been paid to sustainable developments in the field of energy systems [6–8]. The deployment of new technologies, such as Hydrogen-based energy systems [4,9], and Hydrogen and electric vehicles [10,11], besides the renewable energy resources in microgrid (MG) frameworks, have been reported to improve energy system costs and efficiency. On the other hand, reliability concerns of energy systems have been highlighted in recent years [12,13].

Several studies have tried to respond to microgrids (MGs) optimal planning challenges, including Hydrogen-based energy systems, Hydrogen vehicles (HVs), and electric vehicles (EVs) [14,15]. However, there is a research gap in the MGs' optimal reliability-based planning, considering the uncertainties of renewable energy resources and vehicles due to stochastic behaviors of vehicle owners, besides the unavailability of sub-systems under various climatic conditions. This paper aims to fill the discussed gap, which is helpful to overcome the negative impacts of uncertain parts on the MGs' optimal design and planning.

The proposed optimal reliability-based planning of the MGs under various climatic conditions would be helpful to decide about suitable techno-economic decisions about the non-fossil fuel-based vehicles and other energy sources.

1.2. Literature review

1.2.1. MGs' optimal planning without reliability constraints

Much attention has been paid to the optimal planning/designing of energy systems, MGs, and smart grids, including renewable energy sources, new technologies, and energy storage systems (ESSs) [16–18].

In [19], several stand-alone energy systems supplying the intensive energy demand for seawater desalination sites have been investigated to

find the most cost-effective solutions. The optimal sizing, minimizing the total net present cost (TNPC), and CO2 emissions reduction have been concerned. The simulations were carried out using HOMER Pro software, and the results showed that the energy system, including photovoltaic (PV)/wind turbine (WT)/diesel/battery, was the optimum solution for such an application. Elmaadawy et al. [19] concluded that the system TNPC could be reduced up to 81.5% by the suggested optimum solution. However, renewable energy sources' reliability and probabilistic behaviors have not been concerned in this reference. Gomez-Gonzalez et al. [12] reported a new algorithm to optimize the energy management and sub-system sizing of household hybrid PV-based systems, including ESSs. Although it has been noted in Ref. [12] that the system reliability is guaranteed by minimizing the cost of the frequency containment reserve-energy not served, the reliability indices have not been used. The optimum techno-economic sizing for a hybrid MG, including PV units, biomass units, and battery storage system based on the dependency on diesel generators, has been introduced in Ref. [20], while the reliability concerns have not been considered directly.

In none of the discussed references in this sub-section, the reliability aspects have not been concerned with the developed objective function and constraints of the introduced optimization problem. Hence, the MG's reliability requirements might not be met within the results of this type of optimal sizing. Moreover, new aspects, such as Hydrogen-based systems and non-electric vehicles, have not been studied in this category of the available research works.

1.2.2. Optimal reliability-based planning for MGs

The reliability aspects play a crucial role in optimizing energy systems and MGs' optimal planning and operation. Thus, in various studies, reliability-oriented optimization problems have been reported. Anoune et al. [21] tried to introduce a deterministic approach for reducing the investment cost (IC) of hybrid renewable-based energy systems while maintaining a constant temperature for bitumen storage was concerned. It has been reported that obtained results improved the system reliability in Ref. [21], but no discussion was presented about the details in system reliability. Also, the probabilistic behaviors of MG's sub-systems have not been studied. Heidar et al. [22] have studied optimal TNPC-based strategies for MGs, considering weather changes. Reliability-based deterministic and stochastic optimization results in Ref. [22] showed that optimal configuration, including PV/battery/hydropower with optimal capacities, could significantly improve emissions. New optimal planning for a hybrid MG, including PV/WT/diesel/battery, has been investigated by Karrich et al. [23]. The TNPC, CO2 emissions, and penalty cost for greenhouse gas (GHG) subject to loss of power supply probability (LPSP) constraint, as one of the reliability indices, have been concerned in Ref. [23]. Hybrid and off-grid renewable-based energy systems have been studied, besides weather forecasting by artificial neural networks (ANNs) by Ref. [24], while the TNPC, LPSP, and other reliability constraints have been considered. Barakat et al. [25] presented LPSP, the energy expense, and the renewable energy fraction to reduce the GHG emissions for the proposed energy management system of an on-grid rural energy system.

Although different research works have been done in the field of MG's reliability-based optimal sizing of elements and designing, the new energy technologies, like the Hydrogen-based systems and non-electric vehicles, have not been studied. This category of research works in the literature could be extended by adding the discussed new technologies, besides the probabilistic approaches to concern the stochastic behaviors.

1.2.3. Optimal planning for MGs, including hydrogen-based energy systems

Many works of the literature have studied hydrogen-based energy systems [26,27]. In Ref. [28], the game theory (GT) and robust optimization method have been utilized for MGs' optimal energy

Table 1
Summary of the literature about optimal energy management system of MGs.

Ref.	Year	EV	HV	Reliability constraints	Metaheuristic optimization algorithms	Various climatic conditions	EL/HT/FC system	Sensitivity analyses	Hybrid RES	Probabilistic modeling of RES
[22]	2020	–	–	*	–	–	–	*	*	*
[32]	2018	–	–	–	*	–	–	*	*	–
[42]	2020	*	–	–	*	–	*	–	–	–
[41]	2021	–	*	–	–	–	–	–	–	–
[29]	2020	–	–	–	–	*	–	*	*	–
[19]	2020	–	–	*	–	–	–	–	*	–
[44]	2019	–	–	*	*	–	–	*	*	–
[30]	2019	–	–	–	–	–	*	–	*	–
[24]	2019	–	–	*	*	–	*	–	*	–
[25]	2020	–	–	*	*	–	–	–	*	–
[31]	2020	–	–	–	–	–	*	*	*	–
[45]	2019	–	–	*	–	–	*	–	*	–
[46]	2019	*	*	–	–	–	*	*	–	*
[39]	2020	*	*	–	–	–	*	*	–	*
[40]	2020	*	*	–	–	–	–	–	–	*
[35]	2019	*	–	–	–	–	–	*	–	–
[47]	2017	*	–	*	–	–	–	*	*	*
[48]	2018	–	–	*	–	–	*	–	*	–
[37]	2016	*	–	–	*	–	–	–	*	–
[49]	2019	–	–	*	*	–	*	–	*	–
[50]	2021	–	–	*	*	–	–	–	*	–
[51]	2021	–	–	*	–	–	–	*	*	–
[52]	2021	–	–	*	–	–	–	–	*	–
[53]	2021	–	–	*	*	–	–	–	*	*
[54]	2021	–	–	*	*	–	–	*	*	–
[23]	2021	–	–	*	*	–	–	*	*	–
[55]	2021	–	–	–	–	–	–	*	*	–
[56]	2021	–	–	*	–	–	–	–	*	–
[57]	2021	–	–	–	–	–	–	*	*	*
[58]	2021	–	–	*	*	–	–	–	*	–
[59]	2021	–	–	*	*	–	*	*	*	–
[20]	2021	–	–	–	–	–	–	–	*	–
Proposed Study		*	*	*	*	*	*	*	*	*

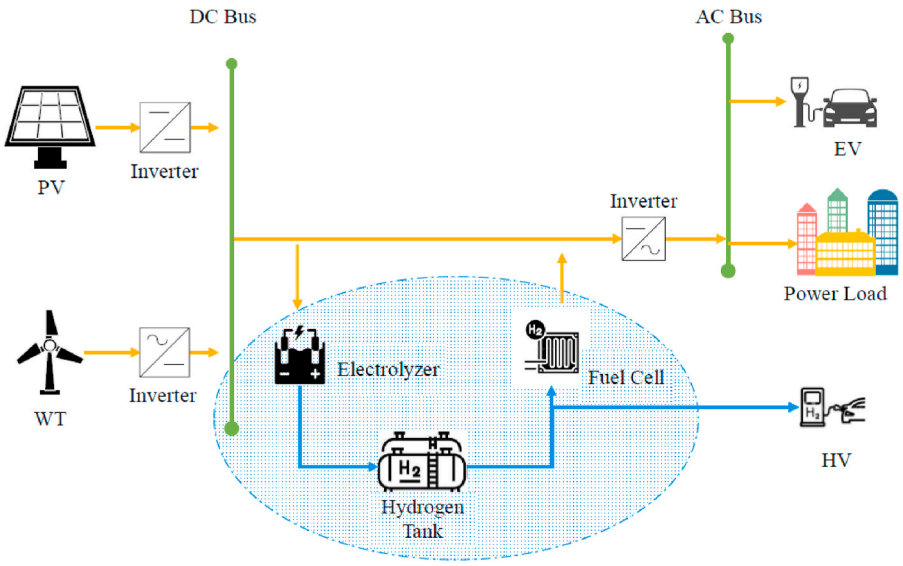

(a) Architecture of the understudy hybrid MG, including the EVs and HVs

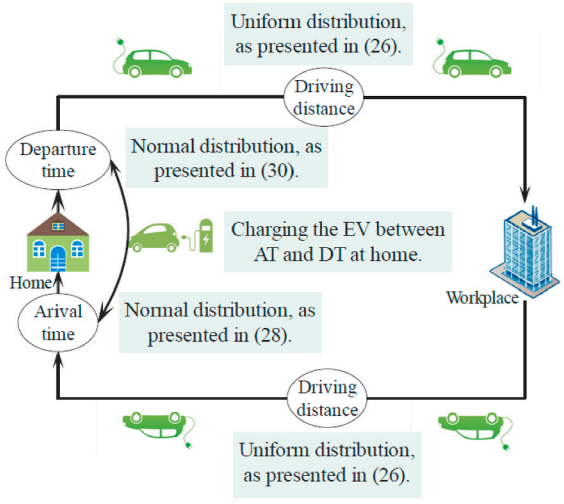

(b) EVs' working cycle

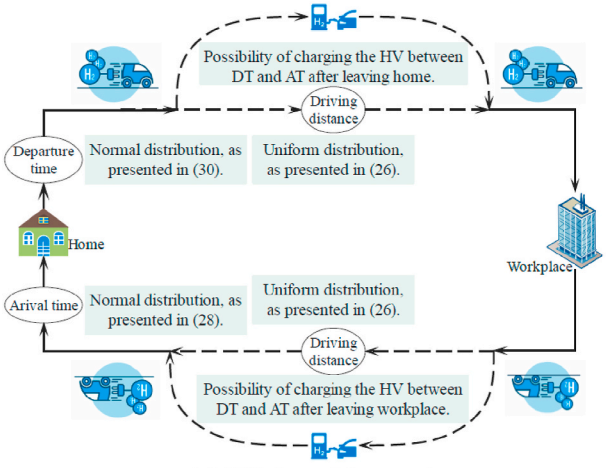

(c) HVs' working cycle

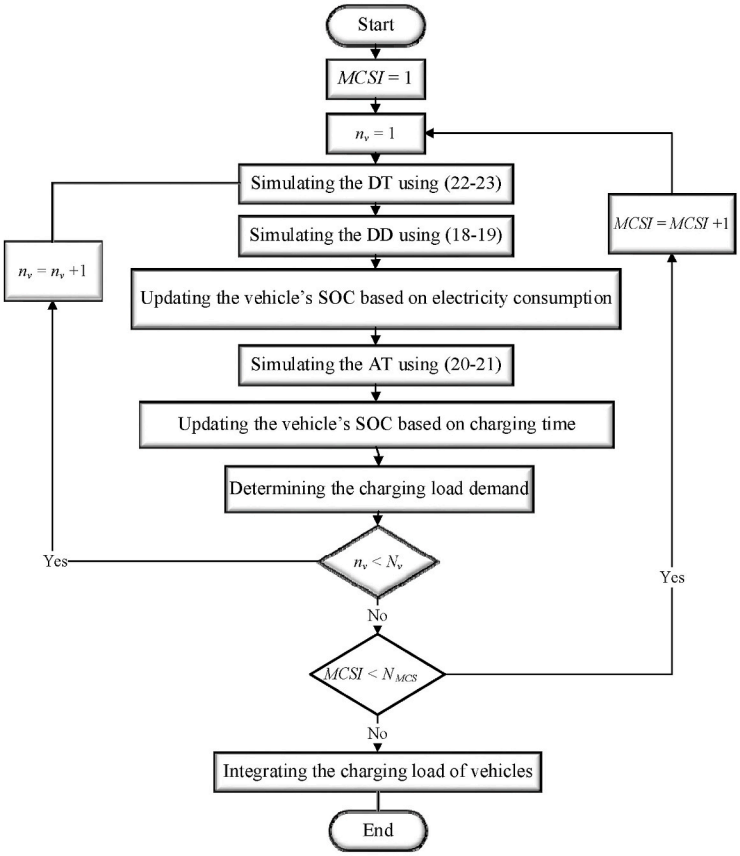

(d) Flowchart of simulating the integrated charging load of vehicles using the MCS

Fig. 1. Structure of the proposed method; (a) architecture of the understudy energy system, (b) conceptual schematic of the working cycle of EVs, (c) conceptual schematic of the working cycle of HVs, (d) flowchart of the simulation process of EVs/HVs integrated charging load by the MCS [97].

management schemes, considering the electricity price uncertainties. In Ref. [29], stand-alone energy systems powered by photovoltaic (PV) and wind turbine (WT) units have been studied. The ESSs have been considered by Rad et al. [29] to supply the energy and water for the residential sector under various climatic conditions. Studying Hydrogen-based systems is one of the advantages of this research. However, the uncertainties of renewable energy resources and reliability constraints have not been concerned, and the reliability constraints were not considered. In Ref. [30], an off-grid energy system has been studied, while the system was equipped with PV panels as its primary power source. Moreover, the hydrogen tank (HT), fuel cell (FC), and electrolyzer (EL) were considered as both ESSs and secondary power sources. In Ref. [31], some optimization problems have been reported to improve the reliability of hybrid renewable-based energy systems using multiple ESS scenarios, e.g., without any ESS, pumped hydro storage system (PHSS), Hydrogen fuel cell (HFC), and hybrid PHSS/HFC ESS. Abdelshafy et al. [32] have studied an off-grid hybrid energy system, including a reverse osmosis desalination system to provide both power and potable water for residential applications. The PV and WT units have been considered the primary source of power, while diesel generators and hydrogen/battery storage systems have been considered the secondary power sources. In Ref. [33], the demand response program (DRP) has been studied in HSS-based MGs. A bi-objective scheduling framework based on economic and environmental aspects has been reported in Ref. [33]. Hadidian et al. [34] introduced a method for MGs, including Hydrogen-based energy system, considering the reliability and uncertainties of MGs' sub-system. However, the EVs, HVs, and impacts of various climates on the advantages of EVs and HVs based on the environmental conditions have not been concerned.

The discussed references in this category are useful to determine how the Hydrogen-based energy systems can improve the optimal planning of MGs. However, some concerns should be added to these available research works, such as studying the impacts of various climates on the effectiveness of Hydrogen-based energy systems, probabilistic modeling, and other new technologies, e.g., HVs and EVs.

1.2.4. Optimal planning for MGs, including HVs and EVs

It has been reported that one of the most effective solutions to mitigate the fossil fuel challenges is to replace conventional fossil fuel-based vehicles with electric vehicles (EVs), plug-in hybrid electric vehicles (PHEVs), and HVs [35,36]. Many countries have encouraged such pollution-free transportation systems [37]. In Ref. [38], an energy system, including EV and PV, was investigated in both grid-connected and islanded operation modes to support a large number of EVs. Xu et al. [39] introduced a new stochastic optimization method to design an optimal MG that is capable of selling electricity and Hydrogen to EVs and HVs. In Ref. [40], the robust non-stochastic programming method has been presented for MGs, which simultaneously supply electricity and Hydrogen for EVs and HVs. İnci et al. [41] have developed cost-effective FC vehicles by vehicle to grid (V2G) mode. In Ref. [42], various energy management strategies and optimum structural designs have been reported to optimize the output power of FC in HVs to increase their operational efficiency and lifetime. Fathabadi [43] presented a fuel cell hybrid electric vehicle (FCHEV), while FC and supercapacitor (SC) hybrid power source was proposed to be used in FCHEV.

The literature review shows that several research works have been done in the areas of EVs and HVs, besides other MGs' aspects. However, the reliability-based optimal planning for MGs, focusing on HVs, under stochastic conditions and various climates, has received less attention.

1.2.5. Literature overview

In Table 1, a brief comparative overview of the literature review has been presented. As seen, although several research works have been done in optimal energy management and planning of the MGs, including RESs, ESSs, EVs, and HVs, a research gap exists about the reliability-based optimal planning of MGs based on the deployment of EVs and HVs under various climates, which considers the probabilistic behaviors simultaneously.

1.3. Contributions and paper organization

This research tries to respond to discussed research gap in the literature by investigating the impacts of the environmental and climatic conditions on the reliability-oriented optimum designs and structures for MGs. Another major contribution is simultaneous stochastic consideration of EVs and HVs, besides other MGs' uncertainties. The proposed optimization problem is solved using the Flower Pollination Algorithm (FPA), and an actual test system has been selected from Iran to illustrate the advantages of the proposed research. The essential contributions of this research could be listed as follows:

- Optimal reliability-based probabilistic design and energy management of the MGs, including the EVs and HVs under various climatic conditions;
- Determining the best solution based on the selection of EVs or HVs for specific climatic conditions;
- Comprehensive probabilistic simulation of EV and HV owners' behaviors, such as arrival time (AT), driving distance (DD), and departure time (DT), besides other system uncertainties.

Other technical features of the proposed study could be itemized as follows to highlight the advantages of this research compared to available references:

- Optimal sizing of the PV, WT, EL, HT, and FC units considering the RESs' uncertainties;
- Examination of the proposed method by studying an MG based on actual historical data of different climates in Iran;
- Investigating the optimal schemes for the studied MG under four climatic conditions;
- Studying the impacts of managed and unmanaged charging of EVs on the MG's energy management system;
- Considering the availability and unavailability of MG's elements;
- Considering the TNPC and reliability constraints in the proposed optimal schemes;
- Sensitivity analyses to evaluate the effects of different loss of energy costs (LOECs)/energy not-supplied cost (ENSC) on the optimal system's TNPC and optimal sizing of MG's elements;
- Sensitivity analyses to get insight into the impacts of the maximum allowed loss of load expected ($LOLE_{max}$) and the maximum allowed loss of energy expected ($LOEE_{max}$) on the optimal TNPC and design variables.

The remainder of this manuscript is structured as follows. In Section 2, the architecture of the understudy hydrogen-based MG is presented. Section 3 consists of the mathematical modeling of the proposed optimization problem. The optimization results, sensitivity analyses, and discussions are given in Section 4. Finally, Section 5 presents the conclusion.

2. Architecture of the understudy MG

The architecture of the understudy MG, including the EVs and HVs, is shown in Fig. 1(a). As seen, the understudy MG includes the PV panels and WTs as its primary sources of power, while the HSS (FC, EL, and HT) works as a backup power supply. The PV and WT units are connected to a DC bus by DC/DC and AC/DC converters, respectively. RES units and FC output power is transformed to AC power using an inverter.

The rules of the proposed energy management system could be described as follows:

- The RESs are considered the primary power sources. The HSS would be in the standby mode if the RESs could supply the MG's loads;
- The surplus energy generated by PV and WT units is stored in the HT using the EL. The constraints of the HT and EL should be considered besides the available energy.
- When the power generated by RESs is insufficient to supply the load demand, the FC starts consuming Hydrogen to generate electrical power. If the output power of the RESs and the available output power of FC could meet the power balance conditions, there is no load curtailment. Otherwise, the MG experiences an interruption.

3. Methods

3.1. Methods for PV units' modeling

The probabilistic behaviors of RESs, such as the output energy of PV units, should be included in the studies [60,61]. This paper uses the Monte Carlo simulation (MCS) to simulate the probabilistic behaviors for solar irradiance and solar clearness index (SCI). A suitable probability distribution should be assigned based on the historical data and statistical analyses. The Beta distribution is an appropriate probability distribution, which could precisely show the probabilistic behaviors of SCI data [62]. A random variable with uniform distribution in the range of [0 1] should be generated in MCS. Then, the inverse of the Beta cumulative density function (CDF) is applied to simulate the SCI, as mathematically expressed in (1) [63,64]. Also, the ambient temperature is another stochastic parameter affecting the output energy of the PV units [65,66]. The Normal distribution can represent the statistical behaviors of the ambient temperature [67]. Hence, it is necessary to simulate the temperature values by the MCS using (2-3).

$$SCI(t) = Inverse \int_{0}^{SCI} \frac{\Gamma(\alpha+\beta)}{\Gamma(\alpha)\Gamma(\beta)} u^{\alpha-1} \ (1-u)^{\beta-1} \tag{1}$$

$$\mathrm{PDF}(T_a) = \frac{1}{\sqrt{2\pi\sigma_{T_a}^2}} \exp\left(- \frac{\left(T_a - \mu_{T_a}\right)^2}{2\sigma_{T_a}^2} \right) \tag{2}$$

$$T_a(t) = Inverse \int_{0}^{T_a} \mathrm{PDF}(T_a, u) \tag{3}$$

The PVs output is a function of solar irradiation/clearness index [68,69]. The output energy of the PV modules could be identified based on (4-8) [70].

$$G(t) = SCI(t) \times G_0 \tag{4}$$

$$T_c(t) = T_a(t) + \left(G(t) \times \frac{(N_{OT} - 20)}{800} \right) \tag{5}$$

$$I_{PV}(t) = SCI(t) \times (I_{sc} + (T_c(t) - T_a(t)) \times K_I) \tag{6}$$

$$V_{PV}(t) = V_{oc} - K_V \times T_c(t) \tag{7}$$

$$P_{PV}(t) = N_{PV} \times I_{PV}(t) \times V_{PV}(t) \times \eta_{PV} \tag{8}$$

3.2. Methods for WTs' modeling

The WTs' output is probabilistic and depends on the wind speed as one of the environmental parameters [71,72]. The Weibull probability distribution has been reported for modeling the statistical behaviors of wind speed in various researches [73]. The wind speed could be simulated by the MCS based on Weibull CDF inverse and generated random variable, as presented in (9) [74].

$$ws = -c_{ws} \ln(u)^{\frac{1}{k_{ws}}} \tag{9}$$

Afterward, the WT output should be determined based on its technical specifications and simulated wind speed by (10) [75].

$$P_{WT}(ws) = \begin{cases} 0 & 0 \le ws < ws_{ci} \\ P_{WT}^{Rated} \times \dfrac{(ws - ws_{ci})}{(ws_{rated} - ws_{ci})} & ws_{ci} \le ws < ws_{rated} \\ P_{WT}^{Rated} & ws_{rated} \le ws \le ws_{co} \\ 0 & ws > ws_{co} \end{cases} \tag{10}$$

Besides the simplified model of the WTs output power, it is possible to use more accurate and detailed models for the WT, as demonstrated in (11).

$$P_{WT}(ws) = \begin{cases} P_{WT-rated} \times \left(A + B \times ws + C \times ws^2\right) & ws_{ci} \le ws < ws_{rated} \\ P_{WT-rated} & ws_{rated} \le ws \le ws_{co} \\ 0 & \text{Otherwise.} \end{cases} \tag{11}$$

The parameters defined in (11), namely A, B, and C, are formulated according to (12)–(14) [76]:

$$A = \frac{1}{\left(ws_{ci} - ws_{rated}\right)^2} \times \begin{bmatrix} ws_{co} \times \left(ws_{ci} + ws_{rated} \right) \\ -4 \times ws_{rated} \times ws_{ci} \left(\dfrac{ws_{ci} + ws_{rated}}{2 \times ws_{rated}} \right)^3 \end{bmatrix} \tag{12}$$

$$B = \frac{1}{\left(ws_{ci} - ws_{rated}\right)^2} \times \begin{bmatrix} 4 \times (ws_{ci} + ws_{rated}) \times \left(\dfrac{ws_{ci} + ws_{rated}}{2 \times ws_{rated}} \right)^3 \\ -(3 \times ws_{ci} + ws_{rated}) \end{bmatrix} \tag{13}$$

$$C = \frac{1}{\left(ws_{ci} - ws_{rated}\right)^2} \times \left[2 - 4 \times \left(\frac{ws_{ci} + ws_{rated}}{2 \times ws_{rated}} \right)^3 \right] \tag{14}$$

It is evident that when the wind speed is between the rated and cut-off speed, the generated power is valued equal to the rated power. The generated power is valued at zero when the wind speed is more than the cut-off or less than the cut-in speeds. Moreover, when the wind speed is between the rated value and the cut-in speeds, there is a second-order polynomial function between the output generation and wind speed.

Both simplified modeling of WT (as shown in (10)) and the more accurate one (as expressed in (11)) can be used. However, the impacts of simplifying the models should be examined.

3.3. Methods for EL's modeling

The EL charges the HT if the generated power by PV and WT units' exceeds the load demand. The EL consumes the electrical power and transforms the water into Hydrogen and Oxygen [77]. In this study, the polymer electrolyte membrane electrolyzer (PEME) [78] has been assumed to be used, and its mathematical modeling is shown in (15-16) [48].

$$P_{EL-HT} = P_{RES-EL} \times \eta_{EL} \tag{15}$$

$$\eta_{EL} = \eta_I \times \eta_V \tag{16}$$

The η_{EL}, η_I, and η_V represent the efficiency of EL, electric current's efficiency, and voltage efficiency, respectively. In the above-discussed modeling, instead of EL's electrical energy demand, the power consumption by the EL in hourly steps according to (15). The amount of produced Hydrogen rate (n_{H_2}) can be shown as (17), where F_{EL} and J_{EL} represent the Faraday constant and the current density, respectively [48].

$$n_{H_2} = \frac{J_{EL}}{2F_{EL}} \tag{17}$$

The required electricity to produce Hydrogen could be formulated as (18) [79].

$$E_{EL}^{elec} = J_{EL} \times V_{EL} \tag{18}$$

In (18), V_{EL} represents the overpotential, and it is achieved through (19), where V_{EL}^{Ohm}, V_{EL}^{0}, $V_{EL}^{Act,c}$, and $V_{EL}^{Act,a}$ denote the ohmic voltage, reversible potential, and the activation overpotential of cathode and anode, respectively [80,81].

$$V_{EL} = V_{EL}^{Ohm} + V_{EL}^{0} + V_{EL}^{Act,c} + V_{EL}^{Act,a} \tag{19}$$

The supplementary explanations and mathematical modeling of parameters and variables in (19) could be found in Refs. [82,83]. Thus, the amount of produced Hydrogen could be distinguished according to its High Heat Value (HHV), based on the Faraday constant and the current density. The introduced modeling for the EL is not simplified, and some essential formulas just have been presented.

3.4. Methods for HT's modeling

The amount of Hydrogen stored in the HT could be determined using (20) [84]. In (20), η_{HT} represents the efficiency of the Hydrogen storage process regarding losses and leakages. Also, Δt denotes simulation time interval. In the simulations, it is necessary to consider that the final stored Hydrogen in the HT should be more than or equal to the initial value, as presented in (21). Moreover, the equivalent mass for stored Hydrogen is calculated using Hydrogen's high heat value based on (22) [85].

$$E_{HT}(t) = E_{HT}(t-1) + P_{EL-HT}(t) \times \Delta t - P_{HT-FC}(t) \times \Delta t \times \eta_{HT} - E_{HV} \tag{20}$$

$$E_{HT}(t = t_0) \le E_{HT}(t = t_0 + 24) \tag{21}$$

$$m_{HT}(t) = \frac{E_{HT}(t)}{HHV_{H_2}} \tag{22}$$

The introduced mathematical model for the HT considers the leakage while the HVs are charged and the losses during the charge/discharge of HT interconnecting EL and FC processes. A proper coefficient (η_{HT}) is used in mathematical modeling for the HT. Due to the power-related nature of the proposed objective function and components' modelings, all of the equations have been presented based on either electrical energy or power. However, the first issue with HT that might be concerned is its storage system and internal pressure and temperature. The temperature and pressure of stored Hydrogen must be considered in both HV and gas stations [86], which this research has not considered.

In addition, the fueling process and the hydrogen pressure during the fueling are other aspects that could be concerned with the more accurate modeling of the HT. The Computational Fluid Dynamics (CFD) modeling, like the model presented in Ref. [87], can be used to examine the impacts of simplified models on the outputs and optimum solutions.

3.5. Methods for FC's modeling

As discussed in the structure of the understudy MG, the FC supplies the loads if the output power of PV and WT units is not sufficient. Indeed, the FC consumes the Hydrogen from the HT, and the electrical power is provided. The proton exchange membrane fuel cell (PEMFC) [88,89] has been considered in this study. In (23), the mathematical modeling of the FC has been described.

$$P_{FC-INV} = P_{HT-FC} \times \eta_{FC} \tag{23}$$

3.6. Methods for Inverter's modeling

The inverter transforms the DC electricity into AC one. The efficiency of the energy conversion by the inverter should be considered using (24).

$$P_{INV-load} = (P_{FC-INV} + P_{RES-INV}) \times \eta_{INV} \tag{24}$$

3.7. Efficiency modeling of sub-systems and elements

It should be noted that the efficiency of components and sub-systems has been assumed to be fixed and constant in this article. However, this assumption itself can cause some levels of uncertainty. In practical cases, the efficiency of elements and sub-systems depends on various operational aspects, such as temperature, electrical outputs, non-electrical outputs, and degradation impacts [90,91]. Hence, further future research works are suggested to examine the changes in the efficiency of elements and sub-systems on the optimum solutions.

3.8. Methods for EVs and HVs' modeling

The understudy MG consists of EVs and HVs. The probabilistic behaviors of vehicle owners affect the charging load demand of EVs and HVs. Hence, it is not possible to precisely study the MG energy management and optimal design without considering the EVs and HVs' uncertainties [92,93]. Furthermore, the stochastic charging load of HVs influences the HT modeling similar to the electrical charging load of EVs [94]. In this paper, the MCS is utilized to concern the uncertainties of AT, DD, and DT for EVs and HVs.

3.8.1. EVs and HVs' DD

By assigning the Log-Normal probability distribution to DD data, it is possible to model the statistical behaviors precisely, as shown in (25) [54]. Hence, the DD could be simulated using the MCS based on CDF inverse and a random variable with uniform distribution, as mathematically expressed in (26).

$$PDF(DD) = \frac{1}{\sqrt{2\pi}\delta_{DD} DD} \exp\left(- \frac{(\ln DD - \mu_{DD})^2}{2\delta_{DD}^2} \right) \tag{25}$$

$$DD = CDF^{-1}(\mu_{DD}, \delta_{DD}, u) \tag{26}$$

3.8.2. EVs and HVs' AT

The home arrival time of EVs and HVs is one of the essential probabilistic parameters affecting the vehicle charging's loads and the MG design and energy management system. The Normal probability distribution is a common alternative for modeling the vehicles' AT, as shown in (27) [95]. The AT should be simulated according to the CDF inverse based on historical data by MCS, as presented in (28).

$$PDF(AT) = \begin{cases} \dfrac{1}{\sqrt{2\pi}\delta_{AT}} \exp\left(- \dfrac{(AT + 24 - \mu_{AT})^2}{2\delta_{AT}^2} \right) & 0 < AT \le \mu_{AT} - 12 \\ \dfrac{1}{\sqrt{2\pi}\delta_{AT}} \exp\left(- \dfrac{(AT - \mu_{AT})^2}{2\delta_{AT}^2} \right) & \mu_{AT} - 12 < AT \le 24 \end{cases} \tag{27}$$

$$AT = CDF^{-1}(\mu_{AT}, \delta_{AT}, u) \tag{28}$$

3.8.3. EVs and HVs' DT

The Normal probability distribution function could represent the statistical behaviors of vehicles' DT, as given in (29) [95]. Similar to other stochastic parameters, the MCS should simulate the DT using the CDF inverse and random variables according to (30).

$$PDF(DT) = \begin{cases} \dfrac{1}{\sqrt{2\pi}\delta_{DT}} \exp\left(- \dfrac{(DT - \mu_{DT})^2}{2\delta_{DT}^2} \right) & 0 < DT \le \mu_{DT} + 12 \\ \dfrac{1}{\sqrt{2\pi}\delta_{DT}} \exp\left(- \dfrac{(DT - 24 - \mu_{DT})^2}{2\delta_{DT}^2} \right) & \mu_{DT} + 12 < DT \le 24 \end{cases} \tag{29}$$

$$DT = CDF^{-1}(\mu_{DT}, \delta_{DT}, u) \tag{30}$$

3.8.4. Integrated charging load of vehicles

Since the behaviors of vehicles are independent, it is possible to simulate the AT, DD, DT, and charging load demand of each vehicle by the MCS. Finally, the charging load of all EVs and HVs could be integrated based on separate charging load demands. In Fig. 1(b), the conceptual schematics of EVs' probabilistic behaviors and their charging are depicted. Fig. 1(c) shows this schematic for HVs' modeling. As seen, the working cycles of EVs and HVs might be different. In addition, the flowchart of the procedure to integrate the stochastic charging loads of EVs using the MCS is shown in Fig. 1(d).

As depicted in Fig. 1(b)–(c), the charging period and charging mechanism of EVs and HVs would be different due to differences between the battery storage system of EVs and the Hydrogen storage system of HVs. The charging period of EVs would be longer than HVs [96]. Moreover, home charging is possible for EVs, while home charging for HVs is not possible. The HVs could be charged between the DT and AT. In this paper, it has been assumed that the HVs would be charged at the parking lots (around 1 h after home departure).

3.9. Methods for reliability modeling of energy resources

In addition to uncertainties of the RES output power, the availability of power sources and power converters influences the MG planning and operation decisions [98]. Considering the reliability modeling of energy resources and converters is one of the most contributions of this study. If it is assumed that all PV and WT units are ideal, the available output power of RES units could be determined using (31), while in realistic conditions, some RES units might be out-of-service.

$$P_{RES}(t) = N_{WT} \times P_{WT}(t) + N_{PV} \times P_{PV}(t) \tag{31}$$

The availability and unavailability of each PV unit and WT unit should be distinguished based on historical data. The available output power of RES could be updated by (32) considering the eventual failures of RES units. In (32), the number of unavailable units has been concerned with updating the available output power.

$$P_{RES}(t) = \left(N_{WT} - n_{WT,F}(t)\right) \times P_{WT}(t) + \left(N_{PV} - n_{PV,F}(t)\right) \times P_{PV}(t) \tag{32}$$

The Binominal is a suitable probability distribution for modeling the availability/unavailability of RES units [99]. The probability of each state based on the specific outage of RES units could be calculated by (33).

$$\Pr\left(n_{WT,F}(t), n_{PV,F}(t)\right) = \begin{bmatrix} \binom{N_{WT}}{n_{WT,F}(t)} \times A_{WT}^{\left(N_{WT}-n_{WT,F}(t)\right)} \\ \times (1-A_{WT})^{n_{WT,F}(t)} \end{bmatrix} \times \begin{bmatrix} \binom{N_{PV}}{n_{PV,F}(t)} \times A_{PV}^{\left(N_{PV}-n_{PV,F}(t)\right)} \\ \times (1-A_{PV})^{n_{PV,F}(t)} \end{bmatrix} \tag{33}$$

Moreover, the failure of inverter units might adversely affect the available energy. Hence, in this study, the failures and unavailability of inverters have also been concerned. In (34), the inverters state would be a Boolean variable, which it's one value that represents the availability of the inverter, and it's zero value means that the inverter is out-of-service. Accordingly, the RES output power could not be delivered to loads if the inverter is unavailable. In addition, the probability of system states based on availability and unavailability of RES and inverter is determined according to (35).

$$P_{RES}(t) = IS(t) \times \begin{bmatrix} \left(N_{WT} - n_{WT,F}(t)\right) \times P_{WT}(t) \\ + \left(N_{PV} - n_{PV,F}(t)\right) \times P_{PV}(t) \end{bmatrix} \tag{34}$$

$$\Pr\left(n_{WT,F}(t), n_{PV,F}(t), IS(t)\right) = \begin{bmatrix} \binom{N_{WT}}{n_{WT,F}(t)} \times A_{WT}^{\left(N_{WT}-n_{WT,F}(t)\right)} \\ \times (1-A_{WT})^{n_{WT,F}(t)} \end{bmatrix} \times \begin{bmatrix} \binom{N_{PV}}{n_{PV,F}(t)} \times A_{PV}^{\left(N_{PV}-n_{PV,F}(t)\right)} \\ \times (1-A_{PV})^{n_{PV,F}(t)} \end{bmatrix} \times \begin{bmatrix} A_{INV}^{IS(t)} \\ \times (1-A_{INV})^{(1-IS(t))} \end{bmatrix} \tag{35}$$

3.10. Proposed objective function (OF)

In this paper, the TNPC, including the cost of MG elements, energy not-supplied cost (ENSC), has been considered for MG's optimal planning and design as presented in (36). The size and capacity of PV units, WT units, EL, HT, and FC, are decision variables in the proposed optimization problems.

$$\text{Min}\{TNPC = NPC_{Com} + NPC_{LOEE}\} \tag{36}$$

As demonstrated in (37), the component costs consist of investment, maintenance, and replacement costs (RCs).

$$NPC_{Com} = C_I + C_{O\&M} + C_{Rep} \tag{37}$$

The IC should be evaluated using (38). The NPC corresponding to operation and maintenance (O&M) costs is also determined by (39-41).

$$C_I = C_{PVs} + C_{WTs} + C_{EL} + C_{HT} + C_{FC} + C_{INV} \tag{38}$$

$$C_{O\&M} = PWA \times \begin{pmatrix} C_{O\&M}^{PVs} + C_{O\&M}^{WTs} \\ + C_{O\&M}^{EL} + C_{O\&M}^{HT} \\ + C_{O\&M}^{FC} + C_{O\&M}^{INV} \end{pmatrix} \tag{39}$$

$$ir = \frac{ir_{nom} - f}{1+f} \tag{40}$$

$$PWA(ir, R) = \frac{(1+ir)^R - 1}{ir(1+ir)^R} \tag{41}$$

In (42), the net present cost corresponding to RCs has been shown.

$$C_{\text{Rep}} = \begin{pmatrix} C_{\text{Rep}}^{PVs} \times \sum_{n=1}^{y_{PV}} \left(\frac{1}{(1+ir)^{n.L_{PV}}}\right) + C_{\text{Rep}}^{WTs} \times \sum_{n=1}^{y_{WT}} \left(\frac{1}{(1+ir)^{n.L_{WT}}}\right) \\ + C_{\text{Rep}}^{EL} \times \sum_{n=1}^{y_{EL}} \left(\frac{1}{(1+ir)^{n.L_{EL}}}\right) + C_{\text{Rep}}^{HT} \times \sum_{n=1}^{y_{HT}} \left(\frac{1}{(1+ir)^{n.L_{HT}}}\right) \\ + C_{\text{Rep}}^{FC} \times \sum_{n=1}^{y_{FC}} \left(\frac{1}{(1+ir)^{n.L_{FC}}}\right) + C_{\text{Rep}}^{INV} \times \sum_{n=1}^{y_{INV}} \left(\frac{1}{(1+ir)^{n.L_{INV}}}\right) \end{pmatrix} \tag{42}$$

In (43-45), the mathematical expression for calculating the LC's NPC has been shown. Also, the coefficient of the present value of the annual payment regarding the LC has been given in (46-47) [100].

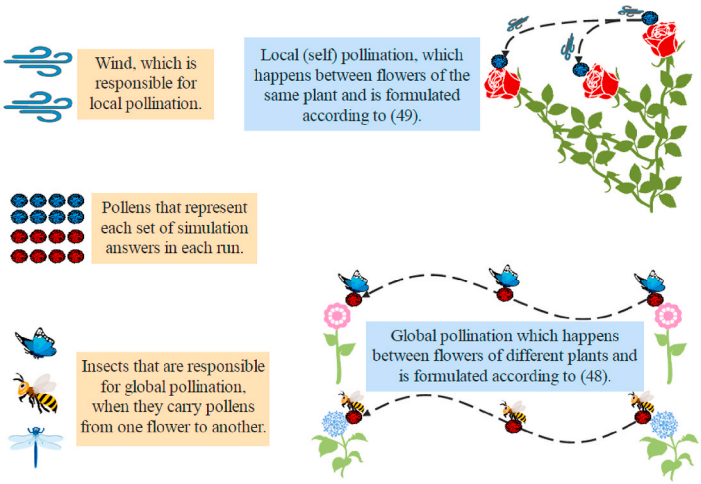

(a) Conceptual schematic of the flower pollination

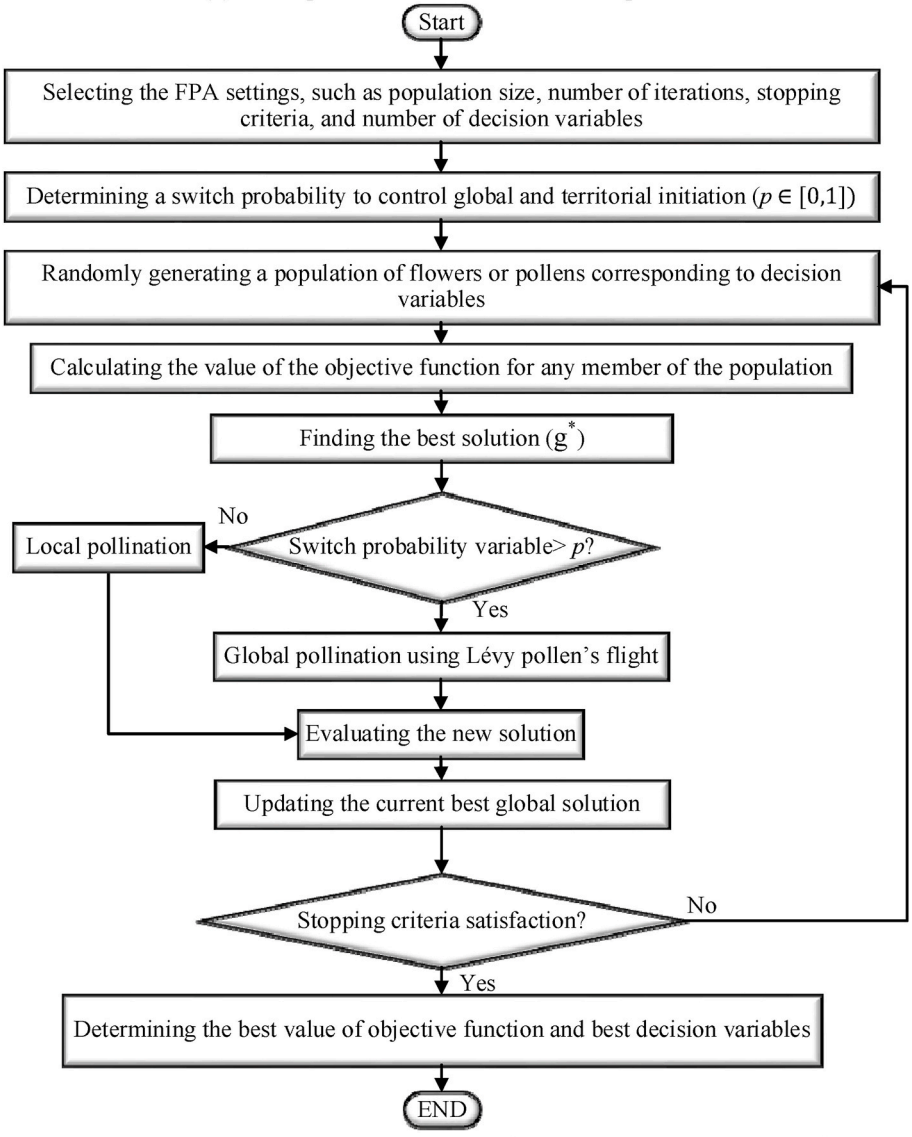

(b) Flowchart of solving the proposed optimization problem using the FPA.

Fig. 2. FPA optimization algorithm; (a) Conceptual schematic of the flower pollination and (b) Flowchart of solving the proposed optimization problem using the FPA.

Table 2
WT characteristics [105,106].

Item	Parameter	Value
1	Type/Model	BWC Excel R/48
2	Rated output power (kW)	7.5
3	IC (USD/unit)	19400
4	O&M cost (USD/unit-year)	75
5	RC (USD/unit)	15000
6	Life-time (year)	20
7	Cut-in speed (m/s)	3
8	Rated speed (m/s)	13
9	Cut-out speed (m/s)	25
10	Maximum number of WTs	300
11	Availability (%)	96

$$LOEE = E\left(\sum_{t} LC(t)\right) \tag{43}$$

$$LOEE \leq LOEE_{\max} \tag{44}$$

$$NPC_{LOEE} = (LOEE \times ENSC) \times PWA(ir, R) \tag{45}$$

$$ir = \frac{ir_{nom} - f}{1 + f} \tag{46}$$

$$PWA(ir, R) = \frac{(1 + ir)^R - 1}{ir(1 + ir)^R} \tag{47}$$

The other lower and upper limits for the capacity of MGs and technical constraints should be concerned in solving the proposed optimization problem.

3.11. Optimization problem solving by Flower Pollination Algorithm (FPA)

The FPA has been selected to solve the proposed optimization problem in this paper. However, it is possible to solve the proposed optimization problem with other algorithms. In Fig. 2(a), the conceptual diagram of natural Flower Pollination has been shown. Also, Fig. 2(b) shows the procedure of solving the optimization problem using FPA.

As seen in Fig. 2(a), a flower's reproduction is carried away by its pollination procedure. A flowering plant spreads its pollens using wind or flying insects in pollination. Self-pollination and cross-pollination are two types of pollination. Cross-pollination occurs between two different flowers where the pollen gets carried from one to another via wind or some insects. In self-pollination, the pollen from one of the flowers in the plant goes to the other flower of the same plant.

The FPA has been developed based on the optimal natural behavior of pollination, while the pollens represent decision variables. As shown in Fig. 2, the population of decision variables (pollens) are generated, and the best value of the objective function is determined by applying the local and global pollination based on the switch probability function. The global pollination could be formulated using (48). Also, the mathematical expression of the local pollination is presented in (49). The i-th and j-th variables are generated randomly, and the ε is selected from a uniform distribution in [0,1] [101].

$$x_l^{FPAI+1} = x_l^{FPAI} + \gamma L(\lambda)\left(g^* - x_l^{FPAI}\right) \tag{48}$$

$$x_l^{FPAI+1} = x_l^{FPAI} + \varepsilon\left(x_i^{FPAI} - x_j^{FPAI+1}\right) \tag{49}$$

Since the introduction of the FPA in 2012, it has been used to optimize a wide variety of optimization problems, such as mixed-integer linear programming (MILP) and mixed-integer nonlinear programming (MINLP) problems based on different OFs and constraints [102–104]. The comparative test results and studies showed that the FPA might have better performance than other optimization algorithms depending on the nature of optimization problems, particularly in MGs' optimization problems. This paper has only focused on the technical features of the proposed optimization problem. However, the performance of solving the optimization problem by other metaheuristic algorithms, e.g., genetic algorithm (GA), Artificial Bee Colony (ABC), and particle swarm optimization (PSO), could be examined in future works.

Table 3
PV characteristics [49,107].

Item	Parameter	Value
1	Rated output power (kW)	1
2	Tracking system	Fixed
3	IC (USD/unit)	7000
4	O&M cost (USD/unit-year)	20
5	RC (USD/unit)	6000
6	Life-time (year)	20
7	Maximum number of PV units	700
8	Availability (%)	96

Table 4
Converter characteristics [49,106].

Item	Parameter	Value
1	IC (USD/unit)	800
2	O&M cost (USD/unit-year)	8
3	RC (USD/unit)	750
4	Converter efficiency (%)	90
5	Life-time (year)	15
6	Rated output power (kW)	1
7	AC output frequency (Hz)	50
8	AC voltage (V)	400
9	DC voltage (V)	48
10	Availability (%)	99.89

Table 5
Hydrogen system's characteristics [49,106].

Item	Unit	Parameter	Value
1	EL	IC (USD/unit)	2000
2		O&M cost (USD/unit-year)	25
3		RC (USD/unit)	1500
4		Efficiency (%)	75
5		Life-time (year)	20
6		Rated output power (kW)	1
7		Availability (%)	100
8		Maximum capacity (kW)	1000
9	HT	IC (USD/unit)	1300
10		O&M cost (USD/unit-year)	15
11		RC (USD/unit)	1200
12		Efficiency (%)	95
13		Life-time (year)	20
14		Availability (%)	100
15		Maximum capacity (kWh)	2000
16	FC	IC (USD/unit)	3000
17		O&M cost (USD/unit-year)	175
18		RC (USD/unit)	2500
19		Efficiency (%)	50
20		Life-time (year)	5
21		Rated output power (kW)	1
22		Availability (%)	100
23		Maximum capacity (kW)	100

4. Test results and discussions

The proposed method for optimal stochastic planning of MGs is applied to a typical test system. The structure of the understudy MG is shown in Fig. 1(a).

In Table 2, the specification of the WT has been demonstrated. The technical and economic specifications for WTs have been extracted from Refs. [105,106]. In addition, the information of PV units has been

Table 6
Specifications of vehicles and their owners' behaviors [94,96,108].

Item	Parameter	Value
1	Total capacity of EV battery (kWh)	30
2	EV electricity consumption (kWh/km)	0.15
3	Min/Max allowable stored electricity in the EV battery (kWh)	3/30
4	Maximum charging/discharging rate of EV (kW)	5
5	Charging/discharging efficiency of EV battery	0.9
6	HV fueling flow rating (kg/min)	1
7	HV fueling/charging time (min)	5
8	HHV_{H2} (kWh/m^3)	39.8
9	HV gasoline equivalent for driving at city (mile/kg)	51
10	Mean of AT (hour)	17.6
11	Variance of AT (hour)	3.4
12	Mean of DT (hour)	8.92
13	Variance of DT (hour)	3.24
14	Mean of DD (km)	3.2
15	Variance of DD (km)	0.88

presented in Table 3 based on [49,107].

The converter is another essential element of the understudy MG, which its characteristics have been shown in Table 4.

The characteristics of the hydrogen system, including the HT, EL, and FC units, have been presented in Table 5.

The technical and economic characteristics of EVs and HVs have been described in Table 6. Moreover, the statistical data for modeling the stochastic behaviors of vehicle owners has been shown. Fig. 3 shows the PDF of vehicle owners' probabilistic behaviors based on historical data. The number of vehicles in the studied MG has been assumed to be 50.

Furthermore, the IEEE RTS load profile with a 50 kW peak value has been considered in this study [109,110].

The proposed optimal planning of the MG, including the EVs and HVs, is studied in the following cases:

- Case No. 1: Desert climate condition
- Case No. 2: Tropical humid climate condition
- Case No. 3: Temperate climate condition
- Case No. 4: Highland climate condition

The historical environmental data of four zones located in Iran with the above climate conditions have been used in this paper. Meibod, Delvar, Nahavand, and Langerood cities have been selected for the desert, tropical humid, highland, and temperate climates, respectively. It should be noted that Iran has six different climates, while desert, tropical humid, highland, and temperate climate zones cover over 94% of its lands. The realistic measured 10-min environmental records [111], which have been transformed into 60-min data, have been used to extract the statistical values for MCS. Iran's Renewable Energy and Energy Efficiency Organization (SATBA) has collected the selected data, which is responsible for renewable energy resources studies and projects in the Iran power ministry. The seasonal statistical values (mean values and standard deviations) for solar irradiance and wind speed in understudy climate conditions have been shown in Figs. 4 and 5, respectively.

Besides investigating four climate conditions, four scenarios based on the deployment of EVs and HVs are studied:

- Scenario No. 1: MG without any EV/HV (like the studies of [34])
- Scenario No. 2: EVs' coordinated charging
- Scenario No. 3: EVs' uncoordinated charging
- Scenario No. 4: HVs' uncoordinated charging

In Scenario 1, it has been assumed that the understudy MG does not consist of EVs/HVs, like the studies of [34]. In Scenarios 2 and 3, the MG should supply the charging loads of EVs under the coordinated and uncoordinated charging modes. Finally, the MG, including HVs, is studied under Scenario 4. It has been assumed that HVs are uncoordinatedly charged because the HVs' home charging would not be possible. Scenario 1 is used to compare with other scenarios to investigate the impacts of EVs/HVs on the MG's TNPC and its optimal sizing and design. Moreover, the effects of coordinated charging and

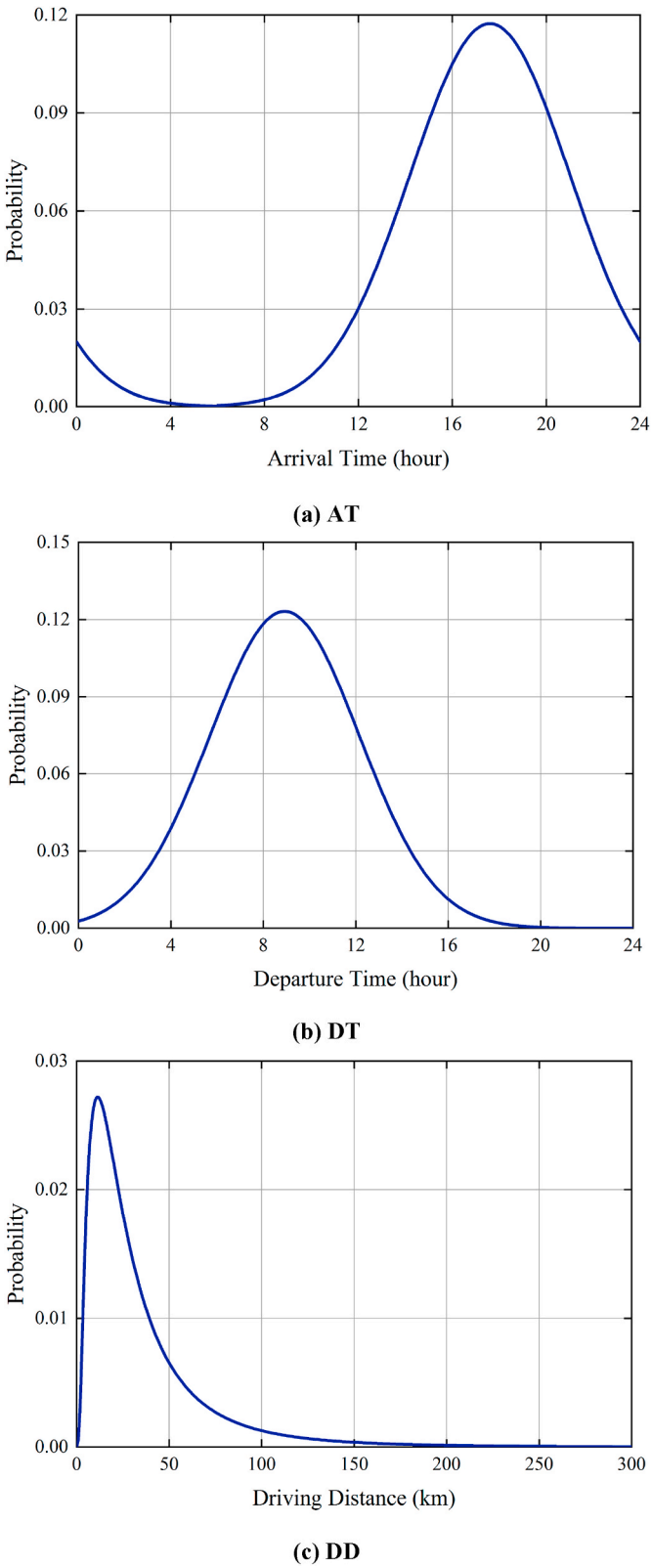

Fig. 3. PDF of probabilistic behaviors of vehicle owners; (a) AT, (b), DT, and (c) DD.

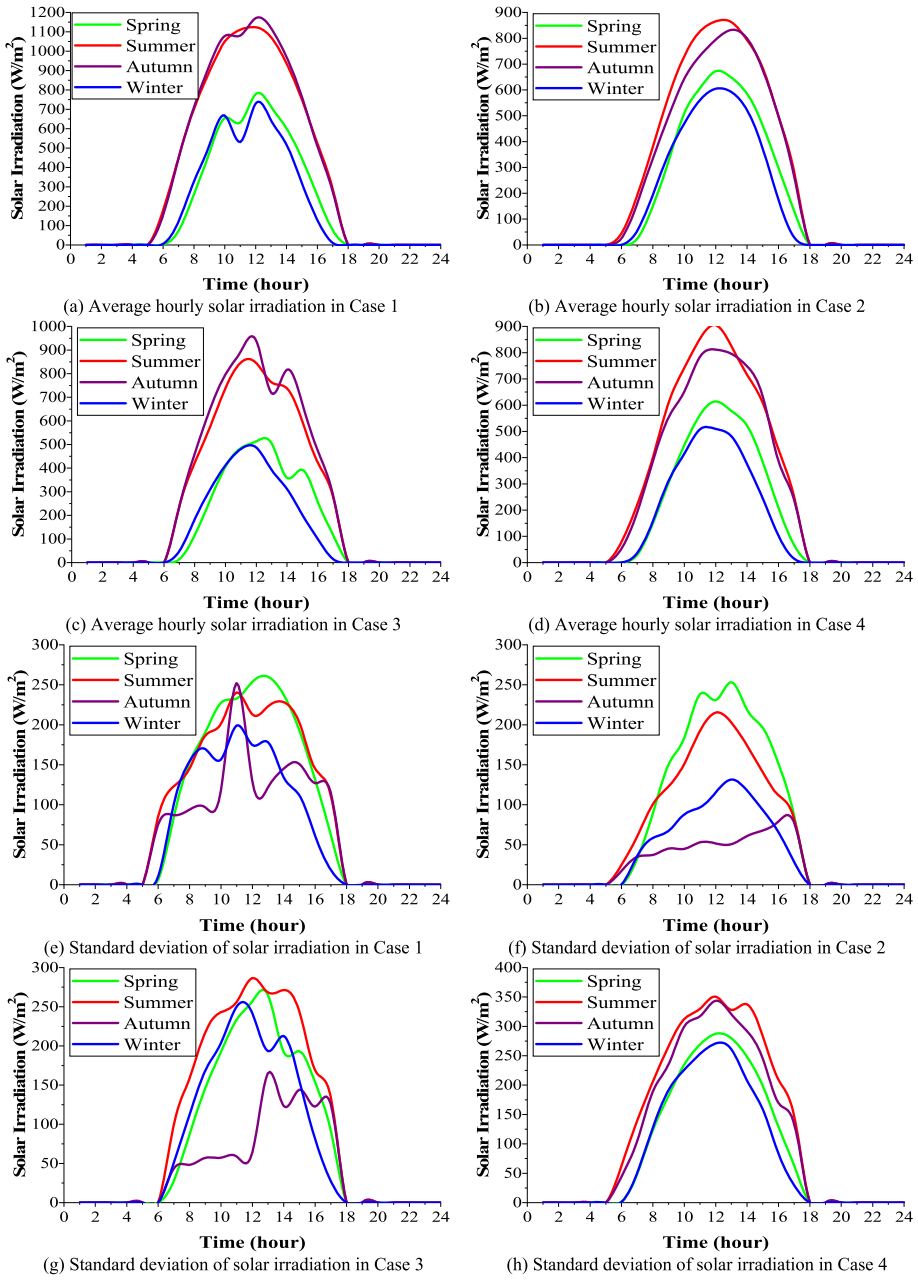

Fig. 4. Seasonal statistical data of solar irradiance in various cases based on historical data of [111].

uncoordinated charging modes are distinguished under Scenarios 2 and 3.

The interest, inflation, and nominal interest rates have been assumed to be 6%, 3%, and 9%, respectively [34].

In this study, ENSC has been considered to be 5.6 USD/kWh, while 1% is considered for the maximum LOLE and LOEE. The proposed method has been implemented in the MATLAB environment.

In Table 7, the optimal results using the deterministic assumptions based on available references like [112,113] have been presented under various cases and scenarios. In addition, the optimal results considering uncertainties of MG parameters by applying the proposed method have been given in Table 8.

The first result that can be concluded from comparing Tables 7 and 8 is that regardless of the cases and scenarios, simplifying assumptions regarding the system uncertainties leads to considerable errors in TNPC. The importance of probabilistic optimal sizing of MGs has been highlighted by comparing the obtained test results.

In Case 1 (desert climate condition), the TNPC's comparisons of considering and neglecting the uncertainties in Tables 7 and 8 show 6.07, 14.71, 12.70, and 14.4% inaccuracies in Scenarios 1, 2, 3, and 4, respectively. The comparative test results illustrate the impacts of stochastic behaviors of MGs' parameters on TNPC.

As revealed by the test result, if the MG does not consist of EVs or HVs, the impacts of uncertainties would be decreased. The minimum inaccuracy in MG's TNPC due to neglecting the system uncertainties has occurred under Scenario 1 (without EVs and HVs). Also, the negative impact of unmanaged charging of EVs on MG's TNPC is another issue, which has been highlighted by comparing test results in Scenarios 2 and 3. Around 10.49% increase in TNPC has occurred due to unmanaged charging of EVs in Case 1. Also, the obtained solutions under Scenarios 2 and 4 infer that the EVs by managed charging strategies could be more economical than HVs for the desert climate zones. If the required infrastructures for coordinating the EVs charging are not available, replacing the EVs with HVs might improve conditions. The TNPC of the

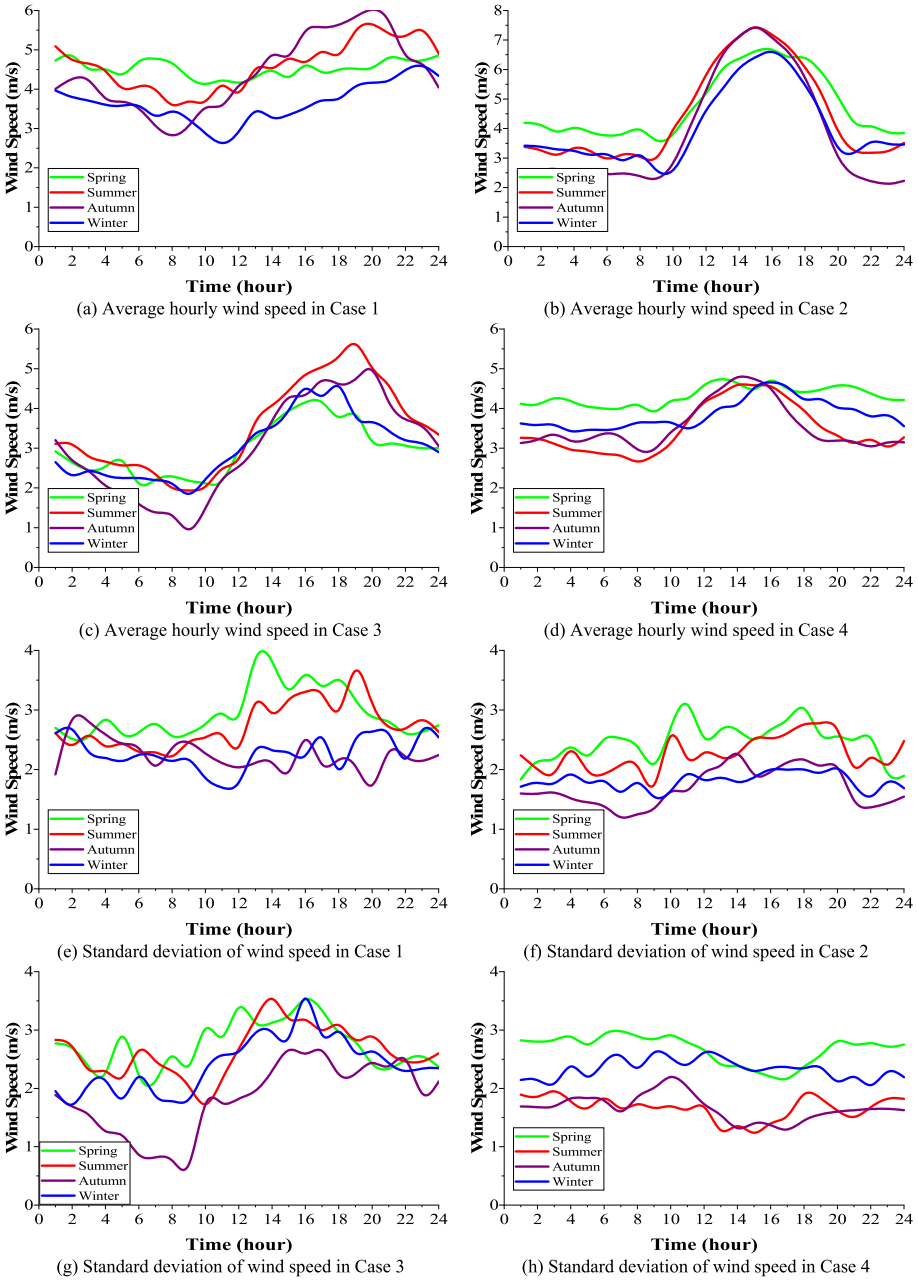

Fig. 5. Seasonal statistical data of wind speed in various cases based on historical data of [111].

MG equipped with HVs is 1.25% less than Scenario 3 (unmanaged charging of EVs). Moreover, the analysis of Case 1 implies that regardless of the vehicle scenarios, the PV units would be more suitable than WTs for desert climates.

The obtained results for Case 1 and comparing the TNPC under Scenario 1 with other scenarios illustrate the significant effects of EVs/HVs charging loads. About 54.27, 70.47, and 68.34 TNPC increments have appeared in Scenarios 2, 3, and 4 compared to Scenario 1 (without considering the EVs/HVs like the studies of [34]). The TNPC increasing under Scenario 3 (unmanaged charging mode of EVs) is expected compared to Scenario 2 (managed charging mode of EVs). The advantages of implementing the charging management strategies for EVs are highlighted based on test results. Moreover, for desert climate conditions, the EVs might have less lead to less energy system cost than HVs.

The TNPC error for neglecting the MG sub-systems' stochastic behaviors in Case 2 would be 4.66%, 9.00, 9.72, and 8.92% for Scenarios 1, 2, 3, and 4, respectively. The impacts of uncertainties in Case 2 (Tropical humid climate condition) are less than in Case 1 (desert climate condition). However, the advantages of the proposed method considering MG uncertainties are also approved in Case 2. Another result highlighted based on the comparison of various scenarios is that adding the EVs and HVs to the MGs intensify the impacts of uncertainties on MGs' TNPC. Test results in Case 2 illustrate the negative impacts of uncoordinated charging of EVs under Scenario 2 compared to Scenario 1 (managed mode for EVs charging). It is concluded that about 10.35% improvement in TNPC would be achievable by coordinating the EVs charging. However, the EVs (under the managed and unmanaged charging modes) would be more appropriate for tropical humid climate zones than HVs. The deployment of more WTs in Case 2 compared to Case 1 is another important conclusion. The comparison of Cases 1 and 2 under various scenarios shows that the TNPC in Case 1 (desert climate condition) could be less than in Case 2 (tropical humid climate condition). It is also concluded that the optimum capacity of HT in Case 2 would be less than other climate cases.

Table 7
Optimal results using the deterministic assumptions, like [112,113], under various cases and scenarios.

Case No.	Scenario No.	TNPC (USD)	N_{WT}	N_{PV}	P_{EL} (kW)	M_{HT} (kg)	P_{FC} (kW)	P_{INV} (kW)
1	1	3,213,110	0	302	143.29	67.72	44.67	46.5
	2	4,501,139	0	452	200.56	83.55	51.82	49.5
	3	5,091,335	0	513	218.73	86.79	72.30	97.34
	4	4,929,142	0	506	228.97	102.76	50.22	49.5
2	1	3,495,885	0	334	163.88	85.61	49.24	49.5
	2	5,021,973	0	526	194.15	87.6	51.72	49.49
	3	5,502,473	0	566	211.06	102.82	71.72	64.55
	4	5,556,708	1	577	217.01	95.28	52.32	99.41
3	1	3,579,273	0	352	154.97	82.78	48.5	49.99
	2	6,016,290	1	656	207.94	92.05	52.33	49.51
	3	6,761,954	0	700	229.19	303.98	67.92	62.52
	4	6,832,705	0	700	230.84	445.61	48.46	100
4	1	3,897,673	0	338	166.87	90.35	49.12	48.5
	2	6,331,248	0	699	215.71	89.34	52.32	49.21
	3	7,395,802	1	700	217.38	752.32	67.95	62.19
	4	7,505,367	0	700	217.43	969.82	48.76	48.10

Table 8
Optimal results of the proposed method considering uncertainties under various cases and scenarios.

Case No.	Scenario No.	TNPC (USD)	N_{WT}	N_{PV}	P_{EL} (kW)	M_{HT} (kg)	P_{FC} (kW)	P_{INV} (kW)
1	1	3,421,015	0	298	175.72	161.54	50.76	49.99
	2	5,277,900	0	544	245.07	170.76	49.19	49.21
	3	5,831,823	0	585	262.66	192.59	67.6	62.52
	4	5,758,910	0	582	263.6	273.83	48.22	67.56
2	1	3,667,091	5	337	174.68	155.48	47.6	48.57
	2	5,523,523	29	504	213.02	74.6	51.28	99.99
	3	6,095,064	29	555	236.76	88.91	70.22	73.77
	4	6,101,246	46	538	220.05	85.77	50.76	96.91
3	1	4,482,977	4	417	225.19	193.33	49.22	49.99
	2	6,762,031	75	498	222.16	291.49	53.41	73.64
	3	7,396,868	82	536	240.82	309.33	71.95	70.16
	4	7,481,432	87	555	279.29	315.46	51.19	49.99
4	1	4,848,659	3	446	262.2	254.22	48.25	92.7
	2	7,417,324	39	697	294.4	157.15	54.44	49.59
	3	8,327,179	58	700	308.05	429.22	66.12	100
	4	8,358,612	59	698	306.75	586.67	47.3	83.03

In Case 2 (tropical humid climate condition), the TNPC increment due to the EVs by the managed charging mode (Scenario 2), unmanaged charging mode of EVs (Scenario 3), and HVs (Scenario 4) compared to Scenario 1 (without considering the EVs/HVs) are 50.62, 66.209, and 68.014%, respectively. The negative impacts of adding the EVs to the MGs in Case 2 for managed and unmanaged charging modes are less than in Case 1, while they are still significant. There is no considerable difference between the negative impacts of HVs on TNPC in Cases 1 and 2.

Around 20.158, 11.02, 8.58, and 8.67% errors might happen due to neglecting the uncertainties in Case 3 under Scenarios 1, 2, 3, and 3, respectively. The maximum deployment of WTs has been suggested in Case 3 compared to other climate cases. In addition, a similar conclusion about the EVs and HVs has been appeared in Case 3, that the managed charging of EVs leads to a better techno-economic situation. The MG's TNPC in Case 3 (temperate climate condition) would be higher than Cases 1 and 2. The maximum capacity for the WTs has been assigned in Case 3. It is approved that the optimal sizing and combination of PV and WT units are affected due to environmental conditions.

The comparison of test results in Case 3 under various scenarios shows that the managed EVs would be a better solution than HVs for highland climate conditions.

In highland conditions (Case 4), the TNPC would be higher than others. As revealed by test results, much more PV units have been suggested in the optimal planning of the understudy MG in Case 4. Test results show that the maximum TNPC occurs in Case 4 and Scenario 3 (highland climate condition and the deployment of HVs), while the minimum TNPC is achievable in Case 2 and Scenario 1 (Tropical humid climate condition and managed charging of EVs).

Regardless of the climate conditions, the significant impacts of the EVs/HVs on the obtained results for the optimal sizing of MGs (based on the comparison of test results under Scenarios 2, 3, and 4 with scenario 1) highlight the advantages of the proposed method in comparison with available studies like the studies of [34], which did not consider the EVs/HVs.

The difference between optimum TNPC for the understudy MGs under various climate conditions is one of the major conclusions of this study. Moreover, test results emphasize that this difference between the TNPC due to climate conditions is highlighted in the presence of EVS/HVs. Test results illustrate that different strategies for optimal sizing of the MGs and the deployment of EVs/HVs should be selected for different climate zones.

Fig. 6 shows the annual load profile, typical charging load of EVs in coordinated and uncoordinated charging modes, and the charging power of HVs. Moreover, the state of energy (SOE) of the HT in various climates under Scenario 4 (using the HVs) is shown in Fig. 6. As seen, the capacity of HT for various climates would be different, while the HT's participation in supplying the loads depends on the climate conditions. Other annual profiles for the demand and supply side could be studied similar to the results shown in Fig. 6.

Considering the reliability constraints is one of the most contributions of this study. Hence, the LOLE and LOEE of a typical one-year period in various cases under different vehicle charging scenarios have been shown in Fig. 7.

As shown in Fig. 7, in Case 1, the most interruptions and inadequacies happened in winter regardless of the vehicle scenarios. This

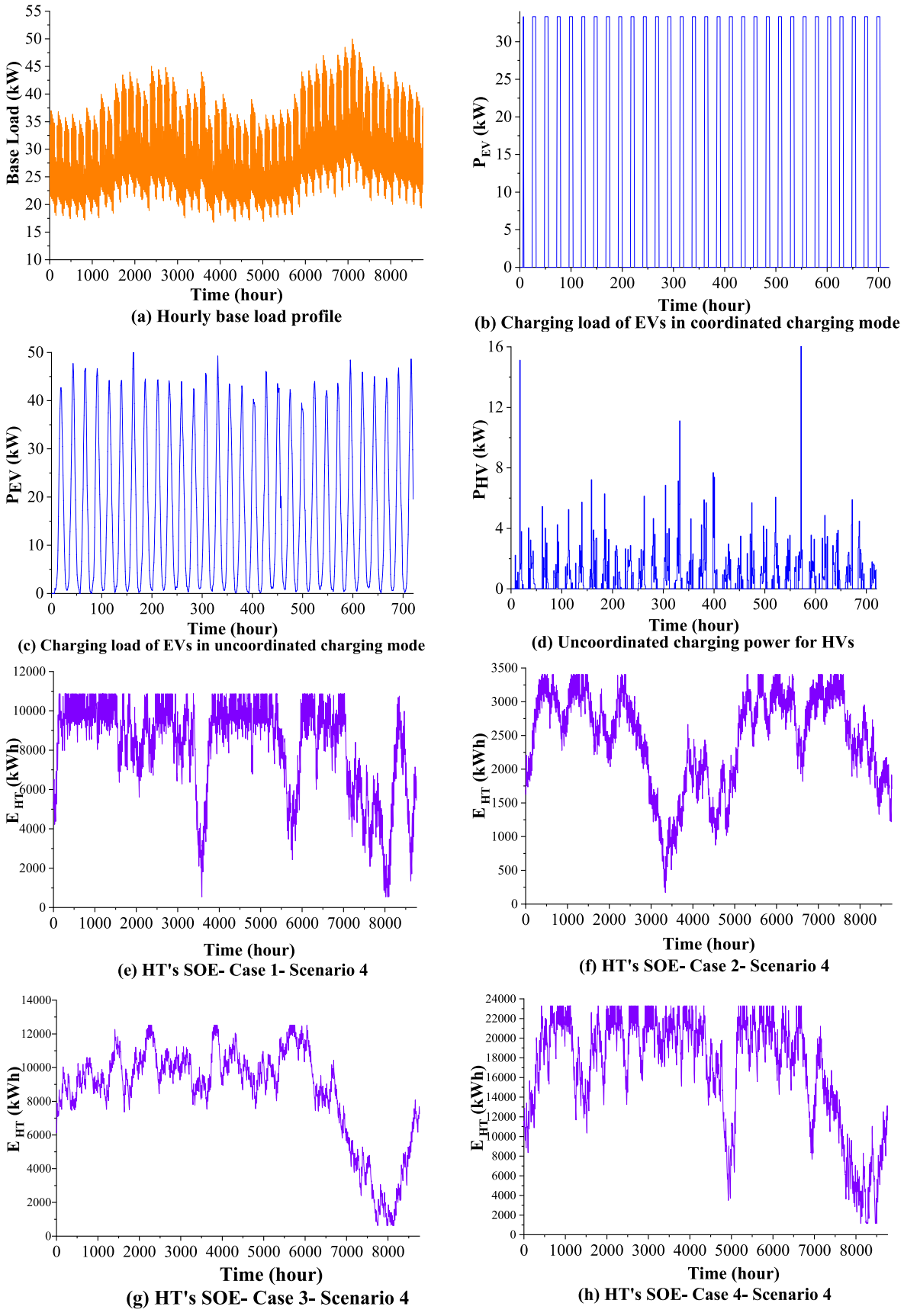

Fig. 6. Load profile, charging load of EVs/HVs, and HT's SOE in various cases under Scenario 4.

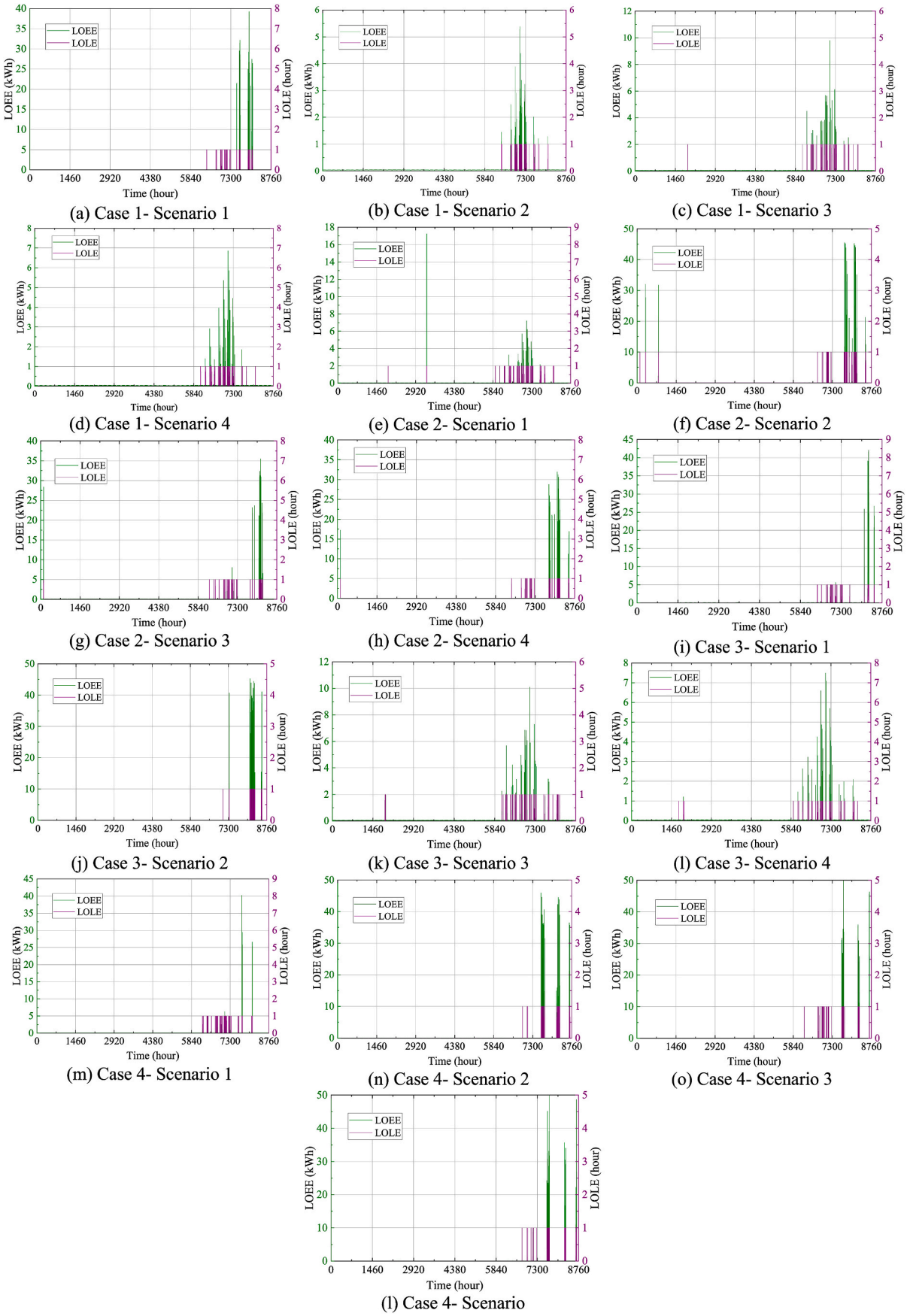

Fig. 7. Hourly LOEE and LOLE in various cases and scenarios, while 1% has been assigned for the maximum allowed LOLE and LOEE.

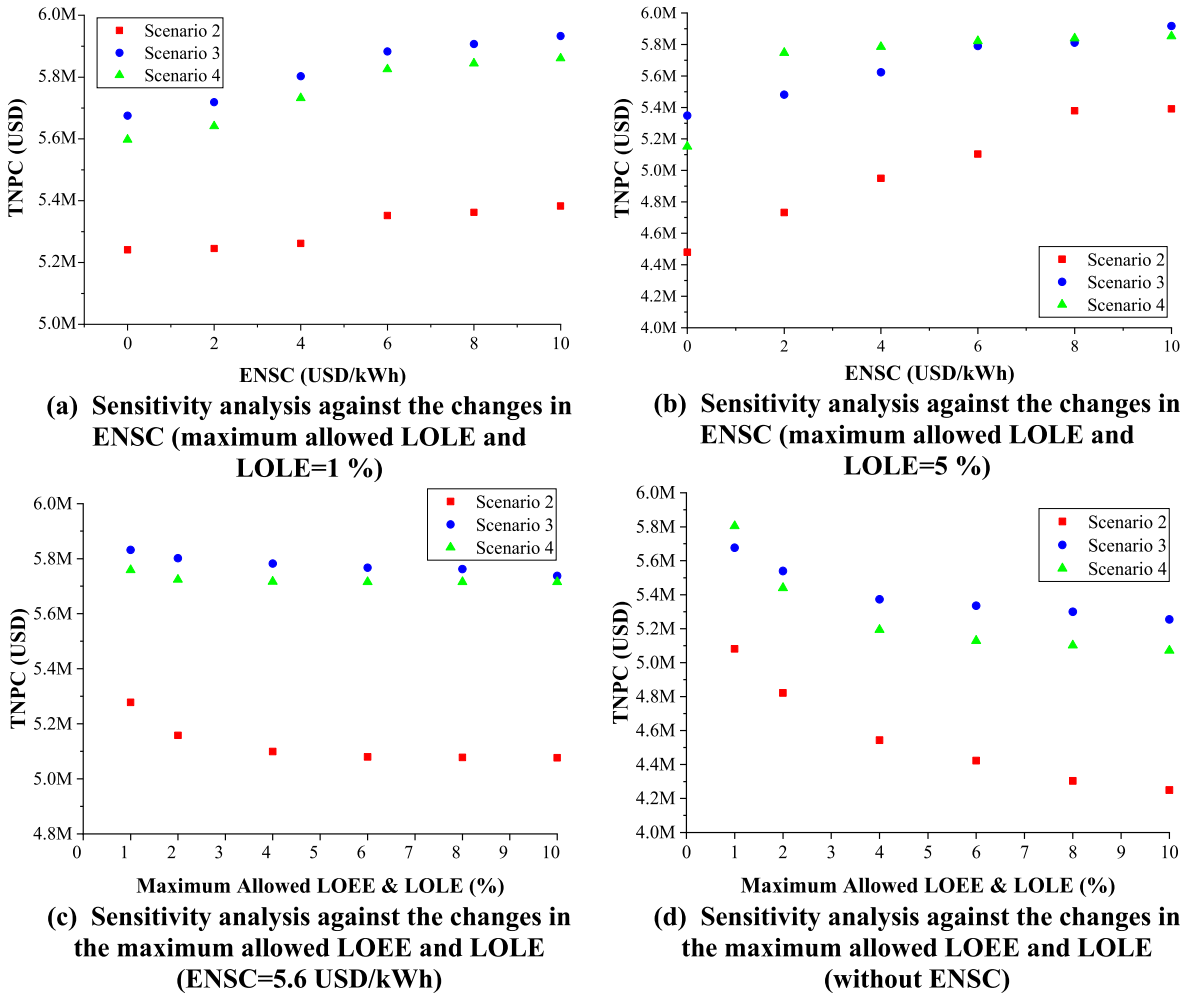

Fig. 8. Sensitivity analyses of TNPC against changes in both ENSC values and the maximum allowed LOEE and LOLE under various scenarios in Case 1.

is mainly because of solar irradiance conditions and load patterns in winter. The maximum hourly load curtailment has occurred under Scenario 3 (uncoordinated charging mode for EVs). In Case 2, the maximum hourly LOEE is approximately similar under various vehicle scenarios. Most of the load interruptions have also appeared in winter for Case 2. Test results of hourly reliability indices in Cases 3 and 4 are also presented in Fig. 7.

The comparative test results of Scenario 1 (without considering the EVs/HVs charging loads like the studies of [34]) with other scenarios shown in Fig. 7 infer that adding the EVs/HVs without considering the required infrastructures and required energy supplied threats the MG's reliability. In addition, the effectiveness and importance of the proposed reliability-based method to optimize the MGs' element sizing and planning are highlighted in the presence of EVs/HVs.

The ENSC is one of the most important reliability parameters influencing MGs' optimized planning and design. Hence, sensitivity analyses have been performed to study the impacts of different ENSC values on the MG's TNPC. In Fig. 8, the sensitivity analyses for different upper bounds of LOEE and LOLE in Case 1 under Scenarios 2, 3, and 4 (including EVs/HVs), as a sample, have been presented. Case 1 has been selected for further discussion because the coverage of this climate is over than others in Iran. However, it is possible to perform similar studies for other cases. As revealed by Fig. 8(a), the impacts of ENSC value on TNPC under Scenario 2 would be less than other scenarios, while 1% has been considered for the maximum allowed LOEE and LOLE. Moreover, regardless of the vehicle scenarios, the changes in TNPC are not significant via changes in the ENSC from 6 USD/kWh to 10 USD/kWh, while the maximum allowed LOEE and LOLE is 1%.

Furthermore, test results in another condition, while the maximum permitted LOEE and LOLE is 5%, as depicted in Fig. 8(b), show that the impacts of ENSC on the MG's TNPC would be intensified for higher upper bounds for reliability indices. It means that the maximum allowed LOEE and LOLE limit the load curtailment, and the reliability costs would not be increased. On the contrary, while the upper bounds for reliability indices are significant, the TNPC and the optimal designs for the MG are affected by the ENSC value. In this condition, the trade-off between the capital and reliability costs due to load curtailments determines the optimum solution.

Fig. 8(c) and (d) show the sensitivity analyses of TNPC via the changes in the upper bounds for LOEE and LOLE in Case 1. Test results illustrate that the TNPC could be decreased if it is possible to increase the upper bounds for reliability indices. It means that much more cost is expected to obtain a more reliable system, particularly for low values of ENSC. However, test results imply that the maximum allowed LOEE and LOLE increment might not affect the TNPC, while the ENSC value is significant. The different behaviors of MG's TNPC via the changes in the maximum allowed LOEE and LOLE for significant ENSC and without considering the ENSC have been presented in Fig. 8.

Another crucial issue is examining the impacts of simplifications in MG's sub-system modeling. Hence, the supplementary studies have been done using the more accurate model for WTs (as shown in (11)) instead of the simplified one (as presented in (10)). Test results inferred that less than 0.709% inaccuracy appears due to simplifying the WT model in the worst case. Similar studies are suggested in further research to

determine the sensitive sub-systems that their accurate models improve the calculations and results.

5. Conclusion

The literature showed a research gap in optimizing the probabilistic designing of MGs, including the RESs, EVs, and HVs in various climate conditions. This research aimed to fill such a gap by reporting a probabilistic reliability-based method, considering the MG uncertainties in the optimal planning of MGs. Considering the EVs and HVs' impacts on the optimal design of the MGs is one of the main contributions. By applying the proposed method, it is possible to determine the best solution between the EVs and HVs for a specified climate zone. The MCS has been used to simulate the stochastic behaviors of vehicle owners and RESs' output power. Also, the proposed optimization problem has been solved using the FPA in the MATLAB environment. The proposed method has been studied under various climates and vehicle charging scenarios. The comparative test results of the proposed probabilistic method and available deterministic ones illustrated that significant inaccuracy occurs due to neglecting the probabilistic behaviors in MGs. It has been concluded that the negative impacts of neglecting the uncertainties of MGs would be highlighted in the uncoordinated charging mode of EVs. However, at least 4.66% of TNPC inaccuracy is inevitable without applying the probabilistic method. In addition, the proposed method, considering the EVs and HVs, has been compared to existing ones, which have not concerned the EVs and HVs. It has been implied that around 50–70% TNPC increment happens due to adding the EVs/HVs to the MG. The maximum TNPC increment belonged to the uncoordinated charging mode of EVs. Furthermore, the sensitivity analyses inferred that the reliability constraints and parameters, e.g., ENSC rate and maximum allowed LOEE and LOLE, might affect the optimized planning of MGs based on their interactions.

The most essential suggested future works to extend this study could be listed as follows:

- Developing the clustering-based and analytical approaches to extend the proposed probabilistic method to improve the computation time of solving the introduced optimization problem;
- Considering the future integrated multi-carrier energy systems (energy hubs), including the heat, cooling, and power to find the optimal planning and design using the proposed reliability-based probabilistic method;
- Studying the grid-connected operation mode, besides the islanded mode of the MG;
- Considering the supplementary objectives in MGs' proposed optimal design and planning, such as customer comfort criteria and environmental and pollution concerns;
- Studying power market-based supportive incentives to apply the obtained optimum solutions in practical applications.

CRediT authorship contribution statement

Mehrdad Aslani: Conceptualization, Methodology, Software, Writing – original draft. **Amir Imanloozadeh:** Conceptualization, Methodology, Software, Writing – original draft. **Hamed Hashemi-Dezaki:** Conceptualization, Methodology, Software, Writing – review & editing, Validation, Supervision. **Maryam A. Hejazi:** Conceptualization, Methodology, Writing – review & editing, Validation. **Mohammad Nazififard:** Conceptualization, Methodology, Writing – review & editing, Validation, Supervision. **Abbas Ketabi:** Conceptualization, Methodology, Writing – review & editing, Validation, Supervision.

Declaration of competing interest

The authors declare that they have no known competing financial interests or personal relationships that could have appeared to influence the work reported in this paper.

References

[1] M. Ram, J.C. Osorio-Aravena, A. Aghahosseini, D. Bogdanov, C. Breyer, Job creation during a climate compliant global energy transition across the power, heat, transport, and desalination sectors by 2050, Energy 238 (2022) 121690, https://doi.org/10.1016/j.energy.2021.121690.
[2] X. Wei, J. Leng, C. Sun, W. Huo, Q. Ren, F. Sun, Co-optimization method of speed planning and energy management for fuel cell vehicles through signalized intersections, J. Power Sources 518 (2022) 230598, https://doi.org/10.1016/j.jpowsour.2021.230598.
[3] Y. Wu, H. Chu, C. Xu, Risk assessment of wind-photovoltaic-hydrogen storage projects using an improved fuzzy synthetic evaluation approach based on cloud model: a case study in China, J. Energy Storage 38 (2021) 102580, https://doi.org/10.1016/j.est.2021.102580.
[4] D. Wang, M. Muratori, J. Eichman, M. Wei, S. Saxena, C. Zhang, Quantifying the flexibility of hydrogen production systems to support large-scale renewable energy integration, J. Power Sources 399 (2018) 383–391, https://doi.org/10.1016/j.jpowsour.2018.07.101.
[5] Y. Cao, X. Zhu, X. Tong, J. Zhou, J. Ni, J. Zhang, J. Pang, Ultrathin microcrystalline hydrogenated Si/Ge alloyed tandem solar cells towards full solar spectrum conversion, Front. Chem. Sci. Eng. 14 (2020) 997–1005, https://doi.org/10.1007/s11705-019-1906-0.
[6] X. Feng, Q. Li, K. Wang, Waste plastic triboelectric nanogenerators using recycled plastic bags for power generation, ACS Appl. Mater. Interfaces 13 (2021) 400–410, https://doi.org/10.1021/acsami.0c16489.
[7] A. Dutta, C.A. Jacob, P. Das, E. Corton, D. Stom, L. Barbora, P. Goswami, A review on power management systems: an electronic tool to enable microbial fuel cells for powering range of electronic appliances, J. Power Sources 517 (2022) 230688, https://doi.org/10.1016/j.jpowsour.2021.230688.
[8] J. Zhao, F. Li, Z. Wang, P. Dong, G. Xia, K. Wang, Flexible PVDF nanogenerator-driven motion sensors for human body motion energy tracking and monitoring, J. Mater. Sci. Mater. Electron. 32 (2021) 14715–14727, https://doi.org/10.1007/s10854-021-06027-w.
[9] T. Egeland-Eriksen, A. Hajizadeh, S. Sartori, Hydrogen-based systems for integration of renewable energy in power systems: achievements and perspectives, Int. J. Hydrogen Energy (2021), https://doi.org/10.1016/j.ijhydene.2021.06.218.
[10] A. Mansour-Saatloo, R. Ebadi, M.A. Mirzaei, K. Zare, B. Mohammadi-Ivatloo, M. Marzband, A. Anvari-Moghaddam, Multi-objective IGDT-based scheduling of low-carbon multi-energy microgrids integrated with hydrogen refueling stations and electric vehicle parking lots, Sustain. Cities Soc. 74 (2021) 103197, https://doi.org/10.1016/j.scs.2021.103197.
[11] I. AlHajri, A. Ahmadian, A. Elkamel, Stochastic day-ahead unit commitment scheduling of integrated electricity and gas networks with hydrogen energy storage (HES), plug-in electric vehicles (PEVs) and renewable energies, Sustain. Cities Soc. 67 (2021) 102736, https://doi.org/10.1016/j.scs.2021.102736.
[12] M. Gomez-Gonzalez, J.C. Hernández, P.G. Vidal, F. Jurado, Novel optimization algorithm for the power and energy management and component sizing applied to hybrid storage-based photovoltaic household-prosumers for the provision of complementarity services, J. Power Sources 482 (2021) 228918, https://doi.org/10.1016/j.jpowsour.2020.228918.
[13] H. Shi, S. Wang, L. Wang, W. Xu, C. Fernandez, B.E. Dablu, Y. Zhang, On-line adaptive asynchronous parameter identification of lumped electrical characteristic model for vehicle lithium-ion battery considering multi-time scale effects, J. Power Sources 517 (2022) 230725, https://doi.org/10.1016/j.jpowsour.2021.230725.
[14] M. Castilla, C. Bordons, A. Visioli, Event-based state-space model predictive control of a renewable hydrogen-based microgrid for office power demand profiles, J. Power Sources 450 (2020) 227670, https://doi.org/10.1016/j.jpowsour.2019.227670.
[15] S. Bracco, F. Delfino, A. Trucco, S. Zin, Electrical storage systems based on Sodium/Nickel chloride batteries: a mathematical model for the cell electrical parameter evaluation validated on a real smart microgrid application, J. Power Sources 399 (2018) 372–382, https://doi.org/10.1016/j.jpowsour.2018.07.115.
[16] K. Wang, C. Liu, J. Sun, K. Zhao, L. Wang, J. Song, C. Duan, L. Li, State of charge estimation of composite energy storage systems with supercapacitors and lithium batteries, Complexity (2021) 8816250, https://doi.org/10.1155/2021/8816250, 2021.
[17] C. Liu, Q. Li, K. Wang, State-of-charge estimation and remaining useful life prediction of supercapacitors, Renew. Sustain. Energy Rev. 150 (2021) 111408, https://doi.org/10.1016/j.rser.2021.111408.
[18] Y. Zhou, Y. Huang, J. Pang, K. Wang, Remaining useful life prediction for supercapacitor based on long short-term memory neural network, J. Power Sources 440 (2019) 227149, https://doi.org/10.1016/j.jpowsour.2019.227149.
[19] K. Elmaadawy, K.M. Kotb, M.R. Elkadeem, S.W. Sharshir, A. Dán, A. Moawad, B. Liu, Optimal sizing and techno-enviro-economic feasibility assessment of large-scale reverse osmosis desalination powered with hybrid renewable energy sources, Energy Convers. Manag. 224 (2020), https://doi.org/10.1016/j.enconman.2020.113377.
[20] A.K. V, A. Verma, Optimal techno-economic sizing of a solar-biomass-battery hybrid system for off-setting dependency on diesel generators for microgrid facilities, J. Energy Storage 36 (2021) 102251, https://doi.org/10.1016/j.est.2021.102251.

[21] K. Anoune, A. Laknizi, M. Bouya, A. Astito, A. Ben Abdellah, Sizing a PV-Wind based hybrid system using deterministic approach, Energy Convers. Manag. 169 (2018) 137–148, https://doi.org/10.1016/j.enconman.2018.05.034.
[22] A.M.A. Haidar, A. Fakhar, A. Helwig, Sustainable energy planning for cost minimization of autonomous hybrid microgrid using combined multi-objective optimization algorithm, Sustain. Cities Soc. 62 (2020) 102391, https://doi.org/10.1016/j.scs.2020.102391.
[23] M. Kharrich, O.H. Mohammed, N. Alshammari, M. Akherraz, Multi-objective optimization and the effect of the economic factors on the design of the microgrid hybrid system, Sustain. Cities Soc. 65 (2021) 102646, https://doi.org/10.1016/j.scs.2020.102646.
[24] W. Zhang, A. Maleki, M.A. Rosen, J. Liu, Sizing a stand-alone solar-wind-hydrogen energy system using weather forecasting and a hybrid search optimization algorithm, Energy Convers. Manag. 180 (2019) 609–621, https://doi.org/10.1016/j.enconman.2018.08.102.
[25] S. Barakat, H. Ibrahim, A.A. Elbaset, Multi-objective optimization of grid-connected PV-wind hybrid system considering reliability, cost, and environmental aspects, Sustain. Cities Soc. 60 (2020) 102178, https://doi.org/10.1016/j.scs.2020.102178.
[26] J. Charvát, P. Mazúr, J. Pocedič, P. Richtr, J. Mrlík, J. Kosek, J. Akrman, L. Kubáč, New organic-air flow fuel cell and electrolyser for stationary energy storage, J. Power Sources 520 (2022) 230811, https://doi.org/10.1016/j.jpowsour.2021.230811.
[27] Z. Feng, J. Huang, S. Jin, G. Wang, Y. Chen, Artificial intelligence-based multi-objective optimisation for proton exchange membrane fuel cell: a literature review, J. Power Sources 520 (2022) 230808, https://doi.org/10.1016/j.jpowsour.2021.230808.
[28] M. Khojasteh, A robust energy procurement strategy for micro-grid operator with hydrogen-based energy resources using game theory, Sustain. Cities Soc. 60 (2020) 102260, https://doi.org/10.1016/j.scs.2020.102260.
[29] M. Amin Vaziri Rad, A. Shahsavari, F. Rajaee, A. Kasaeian, F. Pourfayaz, W. M. Yan, Techno-economic assessment of a hybrid system for energy supply in the affected areas by natural disasters: a case study, Energy Convers. Manag. 221 (2020) 113170, https://doi.org/10.1016/j.enconman.2020.113170.
[30] M. Shaygan, M.A. Ehyaei, A. Ahmadi, M.E.H. Assad, J.L. Silveira, energy, exergy, advanced exergy and economic analyses of hybrid polymer electrolyte membrane (pem) fuel cell and photovoltaic cells to produce hydrogen and electricity, J. Clean. Prod. 234 (2019) 1082–1093, https://doi.org/10.1016/j.jclepro.2019.06.298.
[31] L. Al-Ghussain, R. Samu, O. Taylan, M. Fahrioglu, Sizing renewable energy systems with energy storage systems in microgrids for maximum cost-efficient utilization of renewable energy resources, Sustain. Cities Soc. 55 (2020) 102059, https://doi.org/10.1016/j.scs.2020.102059.
[32] A.M. Abdelshafy, H. Hassan, J. Jurasz, Optimal design of a grid-connected desalination plant powered by renewable energy resources using a hybrid PSO–GWO approach, Energy Convers. Manag. 173 (2018) 331–347, https://doi.org/10.1016/j.enconman.2018.07.083.
[33] S. Seyyedeh-Barhagh, M. Majidi, S. Nojavan, K. Zare, Optimal scheduling of hydrogen storage under economic and environmental priorities in the presence of renewable units and demand response, Sustain. Cities Soc. 46 (2019), https://doi.org/10.1016/j.scs.2018.12.034.
[34] M.J. Hadidian Moghaddam, A. Kalam, S.A. Nowdeh, A. Ahmadi, M. Babanezhad, S. Saha, Optimal sizing and energy management of stand-alone hybrid photovoltaic/wind system based on hydrogen storage considering LOEE and LOLE reliability indices using flower pollination algorithm, Renew. Energy 135 (2019) 1412–1434, https://doi.org/10.1016/j.renene.2018.09.078.
[35] G. Barone, A. Buonomano, F. Calise, C. Forzano, A. Palombo, Building to vehicle to building concept toward a novel zero energy paradigm: modelling and case studies, Renew. Sustain. Energy Rev. 101 (2019) 625–648, https://doi.org/10.1016/j.rser.2018.11.003.
[36] S. Foorginezhad, M. Mohseni-Dargah, Z. Falahati, R. Abbassi, A. Razmjou, M. Asadnia, Sensing advancement towards safety assessment of hydrogen fuel cell vehicles, J. Power Sources 489 (2021) 229450, https://doi.org/10.1016/j.jpowsour.2021.229450.
[37] N. Sujitha, S. Krithiga, RES based EV battery charging system: a review, Renew. Sustain. Energy Rev. 75 (2017) 978–988, https://doi.org/10.1016/j.rser.2016.11.078.
[38] F.M. Eltoumi, M. Becherif, A. Djerdir, H.S. Ramadan, The key issues of electric vehicle charging via hybrid power sources: techno-economic viability, analysis, and recommendations, Renew. Sustain. Energy Rev. 138 (2021) 110534, https://doi.org/10.1016/j.rser.2020.110534.
[39] X. Xu, W. Hu, D. Cao, Q. Huang, W. Liu, M.Z. Jacobson, Z. Chen, Optimal operational strategy for an offgrid hybrid hydrogen/electricity refueling station powered by solar photovoltaics, J. Power Sources 451 (2020) 227810, https://doi.org/10.1016/j.jpowsour.2020.227810.
[40] Y. Wang, M. Kazemi, S. Nojavan, K. Jermsittiparsert, Robust design of off-grid solar-powered charging station for hydrogen and electric vehicles via robust optimization approach, Int. J. Hydrogen Energy 45 (2020) 18995–19006, https://doi.org/10.1016/j.ijhydene.2020.05.098.
[41] M. İnci, M. Büyük, M.M. Savrun, M.H. Demir, Design and analysis of fuel cell vehicle-to-grid (FCV2G) system with high voltage conversion interface for sustainable energy production, Sustain. Cities Soc. 67 (2021), https://doi.org/10.1016/j.scs.2021.102753.
[42] X. Lü, Y. Wu, J. Lian, Y. Zhang, C. Chen, P. Wang, L. Meng, Energy management of hybrid electric vehicles: a review of energy optimization of fuel cell hybrid power system based on genetic algorithm, Energy Convers. Manag. 205 (2020) 112474, https://doi.org/10.1016/j.enconman.2020.112474.
[43] H. Fathabadi, Fuel cell hybrid electric vehicle (FCHEV): novel fuel cell/SC hybrid power generation system, Energy Convers. Manag. 156 (2018) 192–201, https://doi.org/10.1016/j.enconman.2017.11.001.
[44] M. Guezgouz, J. Jurasz, B. Bekkouche, T. Ma, M.S. Javed, A. Kies, Optimal hybrid pumped hydro-battery storage scheme for off-grid renewable energy systems, Energy Convers. Manag. 199 (2019) 112046, https://doi.org/10.1016/j.enconman.2019.112046.
[45] M.R. Akhtari, M. Baneshi, Techno-economic assessment and optimization of a hybrid renewable co-supply of electricity, heat and hydrogen system to enhance performance by recovering excess electricity for a large energy consumer, Energy Convers. Manag. 188 (2019) 131–141, https://doi.org/10.1016/j.enconman.2019.03.067.
[46] H. Mehrjerdi, Off-grid solar powered charging station for electric and hydrogen vehicles including fuel cell and hydrogen storage, Int. J. Hydrogen Energy 44 (2019) 11574–11583, https://doi.org/10.1016/j.ijhydene.2019.03.158.
[47] H. Hashemi-Dezaki, H. Askarian-Abyaneh, A. Shams-Ansari, M. DehghaniSanij, M.A. Hejazi, Direct cyber-power interdependencies-based reliability evaluation of smart grids including wind/solar/diesel distributed generations and plug-in hybrid electrical vehicles, Int. J. Electr. Power Energy Syst. 93 (2017) 1–14, https://doi.org/10.1016/j.ijepes.2017.05.018.
[48] A. Khiareddine, C. Ben Salah, D. Rekioua, M.F. Mimouni, Sizing methodology for hybrid photovoltaic/wind/hydrogen/battery integrated to energy management strategy for pumping system, Energy 153 (2018) 743–762, https://doi.org/10.1016/j.energy.2018.04.073.
[49] M. Jafar, H. Moghaddam, A. Kalam, S. Arabi, Optimal sizing and energy management of stand-alone hybrid photovoltaic/wind system based on hydrogen storage considering LOEE and LOLE reliability indices using fl ower pollination algorithm, Renew. Energy 135 (2019) 1412–1434, https://doi.org/10.1016/j.renene.2018.09.078.
[50] M. Kharrich, S. Kamel, A.S. Alghamdi, A. Eid, M.I. Mosaad, M. Akherraz, M. Abdel-Akher, Optimal design of an isolated hybrid microgrid for enhanced deployment of renewable energy sources in Saudi Arabia, Sustain. Times 13 (2021) 1–26, https://doi.org/10.3390/su13094708.
[51] M.F. Ishraque, S.A. Shezan, J.N. Nur, M.S. Islam, Optimal sizing and assessment of an islanded photovoltaic -battery- diesel generator microgrid applicable to a remote school of Bangladesh, Eng. Reports. 3 (2021) 1–19, https://doi.org/10.1002/eng2.12281.
[52] S. Madhura, V. Boddapati, Optimal sizing and assessment of a hybrid energy based AC microgrid, Mater. Today Proc. (2021), https://doi.org/10.1016/j.matpr.2021.02.133.
[53] L. Zhao, H. Jerbi, R. Abbassi, B. Liu, M. Latifi, H. Nakamura, Sizing renewable energy systems with energy storage systems based microgrids for cost minimization using hybrid shuffled frog-leaping and pattern search algorithm, Sustain. Cities Soc. 73 (2021) 103124, https://doi.org/10.1016/j.scs.2021.103124.
[54] G.K. Suman, J.M. Guerrero, O.P. Roy, Optimisation of solar/wind/bio-generator/diesel/battery based microgrids for rural areas: a PSO-GWO approach, Sustain. Cities Soc. (2021) 102723, https://doi.org/10.1016/j.scs.2021.102723.
[55] J. Graça Gomes, H.J. Xu, Q. Yang, C.Y. Zhao, An optimization study on a typical renewable microgrid energy system with energy storage, Energy 234 (2021) 121210, https://doi.org/10.1016/j.energy.2021.121210.
[56] S. Amara, S. Toumi, C. Ben Salah, A.S. Saidi, Improvement of techno-economic optimal sizing of a hybrid off-grid micro-grid system, Energy 233 (2021) 121166, https://doi.org/10.1016/j.energy.2021.121166.
[57] B.K. Das, M. Hasan, Optimal sizing of a stand-alone hybrid system for electric and thermal loads using excess energy and waste heat, Energy 214 (2021) 119036, https://doi.org/10.1016/j.energy.2020.119036.
[58] A.A. Hafez, A.Y. Abdelaziz, M.A. Hendy, A.F.M. Ali, Optimal sizing of off-line microgrid via hybrid multi-objective simulated annealing particle swarm optimizer, Comput. Electr. Eng. 94 (2021) 107294, https://doi.org/10.1016/j.compeleceng.2021.107294.
[59] M. Approaches, Applied energy prospective Hydrogen-based microgrid systems for optimal leverage via metaheuristic approaches, Appl. Energy 300 (2019) 117384, https://doi.org/10.1016/j.apenergy.2021.117384.
[60] S.M. Hakimi, A. Hasankhani, M. Shafie-khah, J.P.S. Catalão, Stochastic planning of a multi-microgrid considering integration of renewable energy resources and real-time electricity market, Appl. Energy 298 (2021) 117215, https://doi.org/10.1016/j.apenergy.2021.117215.
[61] L.W. Chong, Y.W. Wong, R.K. Rajkumar, D. Isa, An optimal control strategy for standalone PV system with Battery-Supercapacitor Hybrid energy storage system, J. Power Sources 331 (2016) 553–565, https://doi.org/10.1016/j.jpowsour.2016.09.061.
[62] E. Shahrabi, S.M. Hakimi, A. Hasankhani, G. Derakhshan, B. Abdi, Developing optimal energy management of energy hub in the presence of stochastic renewable energy resources, Sustain. Energy, Grids Networks. 26 (2021) 100428, https://doi.org/10.1016/j.segan.2020.100428.
[63] M. Memari, A. Karimi, H. Hashemi-Dezaki, Reliability evaluation of smart grid using various classic and metaheuristic clustering algorithms considering system uncertainties, Int. Trans. Electr. Energy Syst. 31 (2021), e12902, https://doi.org/10.1002/2050-7038.12902.
[64] M. Aslani, H. Hashemi-Dezaki, A. Ketabi, Reliability evaluation of smart microgrids considering cyber failures and disturbances under various cyber network topologies and distributed generation's scenarios, Sustainability 13 (2021) 5695, https://doi.org/10.3390/su13105695.

[65] Y. Cao, C. Liu, J. Jiang, X. Zhu, J. Zhou, J. Ni, J. Zhang, J. Pang, M.H. Rummeli, W. Zhou, H. Liu, G. Cuniberti, Theoretical insight into high-efficiency triple-junction tandem solar cells via the band engineering of antimony chalcogenides, Sol. RRL. 5 (2021) 2000800, https://doi.org/10.1002/solr.202000800.
[66] Y. Cao, X. Zhu, H. Chen, X. Zhang, J. Zhou, Z. Hu, J. Pang, Towards high efficiency inverted Sb2Se3 thin film solar cells, Sol. Energy Mater. Sol. Cells 200 (2019) 109945, https://doi.org/10.1016/j.solmat.2019.109945.
[67] M. Barukčić, Ž. Hederić, M. Hadžiselimović, S. Seme, A simple stochastic method for modelling the uncertainty of photovoltaic power production based on measured data, Energy 165 (2018) 246–256, https://doi.org/10.1016/j.energy.2018.09.134.
[68] J. Zhou, H. Chen, X. Zhang, K. Chi, Y. Cai, Y. Cao, J. Pang, Substrate dependence on (Sb4Se6)n ribbon orientations of antimony selenide thin films: morphology, carrier transport and photovoltaic performance, J. Alloys Compd. 862 (2021) 158703, https://doi.org/10.1016/j.jallcom.2021.158703.
[69] Y. Cao, X. Zhu, J. Jiang, C. Liu, J. Zhou, J. Ni, J. Zhang, J. Pang, Rotational design of charge carrier transport layers for optimal antimony trisulfide solar cells and its integration in tandem devices, Sol. Energy Mater. Sol. Cells 206 (2020) 110279, https://doi.org/10.1016/j.solmat.2019.110279.
[70] H. Hashemi-Dezaki, S.M.M. Agah, H. Askarian-Abyaneh, H. Haeri-Khiavi, Sensitivity analysis of smart grids reliability due to indirect cyber-power interdependencies under various DG technologies, DG penetrations, and operation times, Energy Convers. Manag. 108 (2016) 377–391, https://doi.org/10.1016/j.enconman.2015.10.082.
[71] O. Rubanenko, O. Miroshnyk, S. Shevchenko, V. Yanovych, D. Danylchenko, O. Rubanenko, Distribution of Wind Power Generation Dependently of Meteorological Factors, IEEE KhPI Week Adv. Technol., 2020, pp. 472–477, https://doi.org/10.1109/KhPIWeek51551.2020.9250114, 2020.
[72] A. Hasankhani, S.M. Hakimi, Stochastic energy management of smart microgrid with intermittent renewable energy resources in electricity market, Energy 219 (2021) 119668, https://doi.org/10.1016/j.energy.2020.119668.
[73] J. Wan, F. Zheng, H. Luan, Y. Tian, L. Li, Z. Ma, Z. Xu, Y. Li, Assessment of wind energy resources in the urat area using optimized weibull distribution, Sustain. Energy Technol. Assessments 47 (2021) 101351, https://doi.org/10.1016/j.seta.2021.101351.
[74] M.-R. Yaghoubi-Nia, H. Hashemi-Dezaki, A. Halvaei Niasar, Optimal stochastic scenario-based allocation of smart grids' renewable and non-renewable distributed generation units and protective devices, Sustain. Energy Technol. Assessments 44 (2021), https://doi.org/10.1016/j.seta.2021.101033.
[75] A. Maleki, A. Askarzadeh, Optimal sizing of a PV/wind/diesel system with battery storage for electrification to an off-grid remote region: a case study of Rafsanjan, Iran, Sustain. Energy Technol. Assessments 7 (2014) 147–153, https://doi.org/10.1016/j.seta.2014.04.005.
[76] A.-M. Hariri, H. Hashemi-Dezaki, M.A. Hejazi, A novel generalized analytical reliability assessment method of smart grids including renewable and non-renewable distributed generations and plug-in hybrid electric vehicles, Reliab. Eng. Syst. Saf. 196 (2020) 106746.
[77] G. Yang, S. Yu, Y. Li, K. Li, L. Ding, Z. Xie, W. Wang, Y. Dohrmann, F.-Y. Zhang, A simple convertible electrolyzer in membraneless and membrane-based modes for understanding water splitting mechanism, J. Power Sources 487 (2021) 229353, https://doi.org/10.1016/j.jpowsour.2020.229353.
[78] Z. Kang, S.M. Alia, M. Carmo, G. Bender, In-situ and in-operando analysis of voltage losses using sense wires for proton exchange membrane water electrolyzers, J. Power Sources 481 (2021) 229012, https://doi.org/10.1016/j.jpowsour.2020.229012.
[79] S.M. Alirahmi, M. Rostami, A.H. Farajollahi, Multi-criteria design optimization and thermodynamic analysis of a novel multi-generation energy system for hydrogen, cooling, heating, power, and freshwater, Int. J. Hydrogen Energy 45 (2020) 15047–15062.
[80] O. Bamisile, Q. Huang, J. Li, M. Dagbasi, A.D. Kemena, M. Abid, W. Hu, Modelling and performance analysis of an innovative CPVT, wind and biogas integrated comprehensive energy system: an energy and exergy approach, Energy Convers. Manag. 209 (2020) 112611.
[81] F.A. Boyaghchi, M. Chavoshi, V. Sabeti, Multi-generation system incorporated with PEM electrolyzer and dual ORC based on biomass gasification waste heat recovery: exergetic, economic and environmental impact optimizations, Energy 145 (2018) 38–51.
[82] X. Zhang, R. Zeng, T. Du, Y. He, H. Tian, K. Mu, X. Liu, H. Li, Conventional and energy level based exergoeconomic analysis of biomass and natural gas fired polygeneration system integrated with ground source heat pump and PEM electrolyzer, Energy Convers. Manag. 195 (2019) 313–327.
[83] H. Kianfard, S. Khalilarya, S. Jafarmadar, Exergy and exergoeconomic evaluation of hydrogen and distilled water production via combination of PEM electrolyzer, RO desalination unit and geothermal driven dual fluid ORC, Energy Convers. Manag. 177 (2018) 339–349.
[84] M.Y. El-Sharkh, M. Tanrioven, A. Rahman, M.S. Alam, Cost related sensitivity analysis for optimal operation of a grid-parallel PEM fuel cell power plant, J. Power Sources 161 (2006) 1198–1207, https://doi.org/10.1016/j.jpowsour.2006.06.046.
[85] R. Karki, S. Member, R. Billinton, Reliability/cost implications of PV and wind energy utilization in small isolated power, Systems 16 (2001) 368–373.
[86] L. Zhao, Q. Zhao, J. Zhang, S. Zhang, G. He, M. Zhang, T. Su, X. Liang, C. Huang, W. Yan, Review on studies of the emptying process of compressed hydrogen tanks, Int. J. Hydrogen Energy 46 (2021) 22554–22573, https://doi.org/10.1016/j.ijhydene.2021.04.101.
[87] C. Wen, B. Rogie, M.R. Kærn, E. Rothuizen, A first study of the potential of integrating an ejector in hydrogen fuelling stations for fuelling high pressure hydrogen vehicles, Appl. Energy 260 (2020) 113958, https://doi.org/10.1016/j.apenergy.2019.113958.
[88] B. Zakeri, S. Syri, Electrical energy storage systems: a comparative life cycle cost analysis, Renew. Sustain. Energy Rev. 42 (2015) 569–596, https://doi.org/10.1016/j.rser.2014.10.011.
[89] Q. Wang, B. Li, D. Yang, H. Dai, J.P. Zheng, P. Ming, C. Zhang, Research progress of heat transfer inside proton exchange membrane fuel cells, J. Power Sources 492 (2021) 229613, https://doi.org/10.1016/j.jpowsour.2021.229613.
[90] J. Asenbauer, A. Varzi, S. Passerini, D. Bresser, Revisiting the energy efficiency and (potential) full-cell performance of lithium-ion batteries employing conversion/alloying-type negative electrodes, J. Power Sources 473 (2020) 228583, https://doi.org/10.1016/j.jpowsour.2020.228583.
[91] T. Wang, Q. Li, X. Wang, Y. Qiu, M. Liu, X. Meng, J. Li, W. Chen, An optimized energy management strategy for fuel cell hybrid power system based on maximum efficiency range identification, J. Power Sources 445 (2020) 227333, https://doi.org/10.1016/j.jpowsour.2019.227333.
[92] L. Novoa, J. Brouwer, Dynamics of an integrated solar photovoltaic and battery storage nanogrid for electric vehicle charging, J. Power Sources 399 (2018) 166–178, https://doi.org/10.1016/j.jpowsour.2018.07.092.
[93] W. Wang, Y. Chen, C. Yang, Y. Li, B. Xu, K. Huang, C. Xiang, An efficient optimal sizing strategy for a hybrid electric air-ground vehicle using adaptive spiral optimization algorithm, J. Power Sources 517 (2022) 230704, https://doi.org/10.1016/j.jpowsour.2021.230704.
[94] V. Ananthachar, J.J. Duffy, Efficiencies of hydrogen storage systems onboard fuel cell vehicles, Sol. Energy 78 (2005) 687–694, https://doi.org/10.1016/j.solener.2004.02.008.
[95] X. Lu, Z. Liu, L. Ma, L. Wang, K. Zhou, N. Feng, A robust optimization approach for optimal load dispatch of community energy hub, Appl. Energy 259 (2020), https://doi.org/10.1016/j.apenergy.2019.114195.
[96] M. Tostado-Véliz, P. Arévalo, F. Jurado, A comprehensive electrical-gas-hydrogen Microgrid model for energy management applications, Energy Convers. Manag. 228 (2021), https://doi.org/10.1016/j.enconman.2020.113726.
[97] Q.B. Pham, S.S. Sammen, S.I. Abba, B. Mohammadi, S. Shahid, R.A. Abdulkadir, A new hybrid model based on relevance vector machine with flower pollination algorithm for phycocyanin pigment concentration estimation, Environ. Sci. Pollut. Res. 28 (2021) 32564–32579, https://doi.org/10.1007/s11356-021-12792-2.
[98] J. Faraji, H. Hashemi-Dezaki, A. Ketabi, Stochastic operation and scheduling of energy hub considering renewable energy sources' uncertainty and N-1 contingency, Sustain. Cities Soc. 65 (2021) 102578, https://doi.org/10.1016/j.scs.2020.102578.
[99] S. Nomura, Y. Ohata, T. Hagita, H. Tsutsui, S. Tsuji-Iio, R. Shimada, Wind farms linked by SMES systems, IEEE Trans. Appl. Supercond. 15 (2005) 1951–1954, https://doi.org/10.1109/TASC.2005.849343.
[100] Z. Shi, R. Wang, T. Zhang, Multi-objective optimal design of hybrid renewable energy systems using preference-inspired coevolutionary approach, Sol. Energy 118 (2015) 96–106, https://doi.org/10.1016/j.solener.2015.03.052.
[101] R. Peesapati, V.K. Yadav, N. Kumar, Flower pollination algorithm based multi-objective congestion management considering optimal capacities of distributed generations, Energy 147 (2018) 980–994, https://doi.org/10.1016/j.energy.2018.01.077.
[102] A.Y. Abdelaziz, E.S. Ali, S.M. Abd Elazim, Flower pollination algorithm and loss sensitivity factors for optimal sizing and placement of capacitors in radial distribution systems, Int. J. Electr. Power Energy Syst. 78 (2016) 207–214.
[103] M.M. Samy, S. Barakat, H.S. Ramadan, A flower pollination optimization algorithm for an off-grid PV-Fuel cell hybrid renewable system, Int. J. Hydrogen Energy 44 (2019) 2141–2152.
[104] F.A. Alturki, A.A. Al-Shamma'a, H.M.H. Farh, K. AlSharabi, Optimal sizing of autonomous hybrid energy system using supply-demand-based optimization algorithm, Int. J. Energy Res. 45 (2021) 605–625.
[105] M.J. Khan, M.T. Iqbal, Dynamic modeling and simulation of a small wind-fuel cell hybrid energy system, Renew. Energy 30 (2005) 421–439, https://doi.org/10.1016/j.renene.2004.05.013.
[106] A. Kashefi Kaviani, G.H. Riahy, S.M. Kouhsari, Optimal design of a reliable hydrogen-based stand-alone wind/PV generating system, considering component outages, Renew. Energy 34 (2009) 2380–2390, https://doi.org/10.1016/j.renene.2009.03.020.
[107] H. Yang, W. Zhou, L. Lu, Z. Fang, Optimal sizing method for stand-alone hybrid solar-wind system with LPSP technology by using genetic algorithm, Sol. Energy 82 (2008) 354–367, https://doi.org/10.1016/j.solener.2007.08.005.

[108] X. Lu, K. Zhou, S. Yang, H. Liu, Multi-objective optimal load dispatch of microgrid with stochastic access of electric vehicles, J. Clean. Prod. 195 (2018) 187–199, https://doi.org/10.1016/j.jclepro.2018.05.190.
[109] P.M. Subcommittee, IEEE reliability test system, IEEE Trans. Power Appar. Syst. PAS- 98 (1979) 2047–2054, https://doi.org/10.1109/TPAS.1979.319398.
[110] M. Kamruzzaman, M. Benidris, Reliability-based metrics to quantify the maximum permissible load demand of electric vehicles, IEEE Trans. Ind. Appl. 55 (2019) 3365–3375, https://doi.org/10.1109/TIA.2019.2914877.
[111] Renewable Energy and Energy Efficiency Organization of Iran, Wind Speed and Radiation Data Sheets [Online]. Available: http://www.satba.gov.ir/en/regions.
[112] M. Amini, A. Khorsandi, B. Vahidi, S.H. Hosseinian, A. Malakmahmoudi, Optimal sizing of battery energy storage in a microgrid considering capacity degradation and replacement year, Elec. Power Syst. Res. 195 (2021) 107170, https://doi.org/10.1016/j.epsr.2021.107170.
[113] M.M. Gamil, T. Senjyu, H. Takahashi, A.M. Hemeida, N. Krishna, M.E. Lotfy, Optimal multi-objective sizing of a residential microgrid in Egypt with different ToU demand response percentages, Sustain. Cities Soc. 75 (2021) 103293, https://doi.org/10.1016/j.scs.2021.103293.